HyDiaD: A hybrid species distribution model combining dispersal, multi-habitat suitability, and population dynamics for diadromous species under climate change scenarios

Betsy Barber-O'Malley [a,b,1], Géraldine Lassalle [a,*], Guillem Chust [c], Estibaliz Diaz [c], Andrew O'Malley [b,1], César Paradinas Blázquez [d], Javier Pórtoles Marquina [d], Patrick Lambert [a]

[a] INRAE, UR EABX, 50 avenue de Verdun, Gazinet-Cestas, 33612 France
[b] University of Maine, 168 College Avenue, Orono, ME 04469, United-States
[c] AZTI Marine Research, Basque Research and Technology Alliance (BRTA), Txatxarramendi Ugartea z/g, Sukarrieta, 48395 Spain
[d] FIC, Fundación para la Investigación del Clima, Gran Vía, 22, Madrid, 28013, Spain

ABSTRACT

Diadromous species are particularly vulnerable to climate change because they utilize both marine and freshwater habitat to complete their life cycles. Dispersal plays an important role in restraining the distribution of plant and animal species, and is a key mechanism to allow diadromous species to adapt to changes in habitat suitability, but it is often not included in species distribution models that explore population trends under climate scenarios. The objective of this study was to develop a model to estimate potential shifts in diadromous populations in the Atlantic area of Europe under two climate change scenarios and multiple global climate models. To address the question of range-shift responses, a hybrid approach for diadromous species distribution (HyDiaD) was developed that incorporated two components: i) statistical static models of habitat suitability describing the influence of environmental factors on species occurrence, and ii) biological processes relevant for the distribution of the species, such as population demography and dispersal dynamics. Hybrid models were developed using a novel approach that incorporated both population and between-catchment dispersal dynamics specific to each species. Occupancy data for diadromous species in a subset of Atlantic Area catchments were first validated by regional experts, and boosted regression trees were applied to estimate habitat suitability within each catchment based on historical physical and climatic environmental predictors from the continental and marine domains. Habitat suitability was then used in a population dynamics model that incorporated between-catchment dispersal and local population growth. Results for different-sized catchments were compared using time series of spawner density and saturation rate, which estimated how much of the available habitat was being utilized. Many of the species-specific values used in HyDiaD were estimated through a survey of diadromous species experts, and group consensus was reached by calculating weighted averages. The HyDiaD model was applied to two shad species (*Alosa alosa* and *A. fallax*) to explore population trends projected annually from 1951 to 2100. Projected trends indicated that under XXIst century climate scenarios, habitat suitability is expected to increase for *A. fallax*, but decrease for *A. alosa*. Projected trends also indicated an increase in the rate of annual variability for *A. alosa*, particularly in the southern part of its range. Future studies can utilize the HyDiaD model to explore distribution trends for other diadromous species under climate change scenarios.

1. Introduction

Diadromous species that migrate between marine and freshwater habitats (McDowall 1988) are especially vulnerable to climate change due to their complex life cycle. Diadromous species experience the effects of changes in climate conditions in both domains and across different life stages (Robinson et al., 2011; Hare et al., 2016; Lin et al., 2017), potentially through a latitudinal range shift in species

---

distributions (Perry et al., 2005; Dambach and Rödder, 2011). It is challenging to develop a better understanding and accurate estimation of the potential effect of climate changes on diadromous species because they utilize both freshwater and marine habitat. Correlative Species Distribution Models (C-SDMs), which are based on the generalized relationships between observed presences/absences and abiotic environmental parameters (Guisan and Zimmermann, 2000), have been implemented for a large number of species to address the possible effect of climate change. However, C-SDMs do not take into account biological factors that are considered important for estimating species distributions, such as population dynamics and dispersal capacity (Guisan and Thuiller, 2005; Elith et al., 2010; Fordham et al., 2013; Melo-Merino et al., 2020). On the other end of the spectrum, mechanistic species distribution models (M-SDMs) explicitly account for these dynamics by incorporating how both abiotic and biological processes constrain the distribution and abundance of a species (Kearney and Porter, 2009; Singer et al., 2016). However, M-SDMs require greater computer processing power and more detailed datasets to parameterize (Fordham et al., 2018), and so have generally only been calibrated for well-studied or commercially exploited species for which physiological or ecological constraints are known(Kearney and Porter, 2009; Cheung et al., 2010; Rougier et al., 2014; Lotze et al., 2019). Developing M-SDMs for data-poor diadromous species on a large spatial scale is problematic because large number of parameters to estimate with insufficient data can trigger high uncertainty.

A hybrid species distribution model (H-SDM) approach could be classified as intermediate between correlative and mechanistic species distribution models in terms of both model complexity (i.e. number of parameters) and data requirements (Singer et al., 2016). H-SDMs include two components: i) the correlation of species observations with abiotic environmental conditions, and ii) biological processes relevant for the distribution of the species, such as population demography, predator-prey interactions, and dispersal dynamics (Dormann et al., 2012; Singer et al., 2018). Different studies have shown that incorporating both of these components has led to an improvement in the estimates of species distributions and potential range shifts compared to only including abiotic environmental conditions (Latimer et al., 2006; Dormann et al., 2012; Fordham et al., 2013; Singer et al., 2018). These hybrid models first determine the presences or absences of a species taking into account environmental conditions, then biological factors, thereby incorporating spatially-explicit processes that act on both a coarser and finer spatial scale (Boulangeat et al., 2012).

Regarding biological factors, dispersal is a key mechanism driving the range-shift response of aquatic organisms to climate change by increasing population resilience through metapopulation or source-sink dynamics (Harrison, 1991; Hanski, 1998). Individuals within a population may return to spawn in the location where they originated (homing), or they may disperse to a non-natal catchment to participate in reproduction (straying; Quinn (1993)). Methodological and data limitations have resulted in many previous niche-based modeling studies that assumed no dispersal or unlimited dispersal (Guisan and Thuiller, 2005; Lassalle et al., 2008b; Franklin, 2010; Holloway and Miller, 2017), but these two hypotheses overestimated either the range loss or the species' dispersal abilities (Jaeschke et al., 2013). These hypotheses are simple decision rules on whether a newly suitable environment is reachable or not. At the population scale, straying and source/sink dynamics may provide a mechanism for recovery after poor year-class recruitment or may be a way for diadromous species to face environmental changes such as habitat fragmentation and loss (Schtickzelle and Quinn, 2007). However, this possible "rescue effect" (i. e. emigrants from surrounding populations reduce the local extinction occurrence (Gotelli, 1991)) of strayers moving from source to sink populations may only persist when overall productivity is relatively high, as suggested from simulated populations of Atlantic salmon (*Salmo salar*) (Bowlby and Gibson, 2019). Another factor that may interact with dispersal in shaping species response to environmental changes is the Allee effect (Stephens and Sutherland, 1999). This concept is defined as a positive relationship between population density and the per capita growth rate of a population. Previous studies have suggested that this effect can prevent recovery of marine fish populations at low abundances (Rougier et al., 2012; Hutchings, 2014; Kuparinen et al., 2014; Perälä and Kuparinen, 2017), and climate change is anticipated to strengthen these effects (Berec, 2019; Winter et al., 2020).
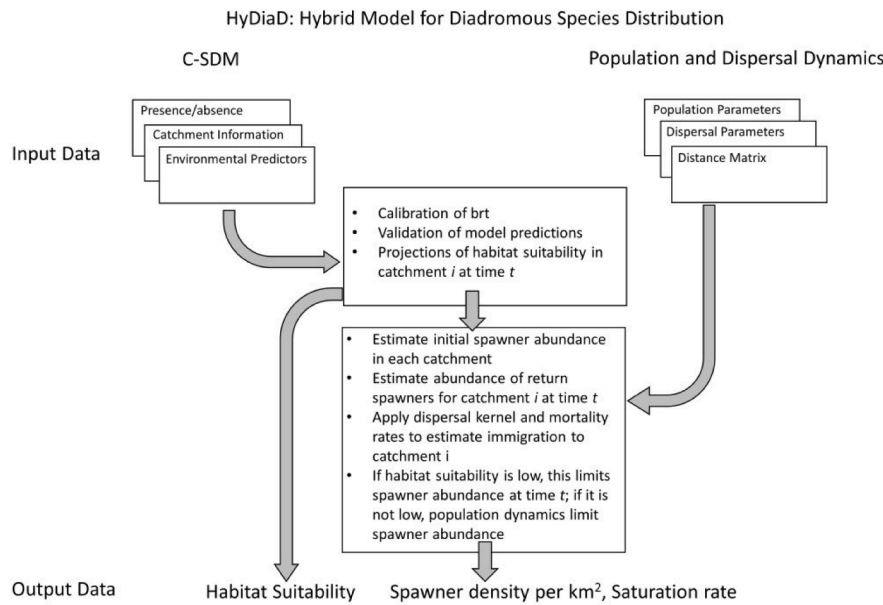
The primary objective of this study was to develop an original H-SDM framework for diadromous species that incorporated dispersal and population dynamics coupled with a habitat suitability module based on environmental predictor variables from both marine and freshwater habitats. This new modeling framework, named HyDiaD for "**Hy**brid approach for **Dia**dromous species **D**istribution", could be utilized for various diadromous species despite differences in distributions and life-history types. These models were intended to improve upon the existing C-SDMs developed for European diadromous species by Lassalle et al. (2008b) and Lassalle and Rochard (2009), which assumed unlimited dispersal (i.e. all newly predicted suitable habitats were reachable) and only included environmental predictor variables from the freshwater habitat. HyDiaD was developed using the steps in the H-SDM modeling framework outlined in Singer et al. (2018) for species with common life-history strategies in continuous terrestrial environments. As recommended by the previous authors, knowledge gaps were identified, and an expert elicitation procedure was designed to provide group-based estimates of missing parameters for Western European diadromous species. The dispersal process in HyDiaD was developed taking into account spatial units (i.e. here catchments compared to grid cells) that were varying sizes and distances apart within a spatial matrix that included both the freshwater and oceanic domains. The secondary objective was to apply HyDiaD to the two Western European shads, the allis shad *Alosa alosa* and the twaite shad *A. fallax*, to project species distribution trends under multiple XXIst climate models.

2. Material and methods

HyDiaD was developed to simulate shifts in habitat suitability related to changes in environmental predictors, dispersal processes, and population dynamics that were specific to each species (Fig. 1). HyDiaD was developed using the steps in the H-SDM modeling framework outlined in Singer et al. (2018) for species with common life-history strategies in continuous terrestrial environments. The first step is the habitat modeling by correlating species occurrences with abiotic conditions (Section 2.2). The second step consists in inserting population dynamics processes, accounting for both demography and dispersal, with a strong emphasis put on reducing knowledge gaps (Section 2.3). The advantages of a hybrid approach was assessed by comparing outputs from the habitat model alone (first step of the HyDiaD framework) with outputs when biological processes were included in the HyDiaD framework (second step fo the HyDiaD framework). Nonetheless, the application of the Singer et al. (2018) generic method to diadromous species required several methodological developments that are fully presented below, including i) the use of a connectivity matrix to estimate distance between pairs of catchments based on shortest aquatic path, ii) the estimation of population dynamics parameters and dispersal kernel through an expert knowledge survey, iii) the estimation of among-catchment dispersal dynamics, iv) the calculation of spawner abundance based on catchment size and species-specific spawner density rather than probability of occupancy, and vii) the use of multiple Global Climate models (GCMs) and Representative Concentration Pathway (RCP) scenarios to project spawner abundance. The source code was provided at https://doi.org/10.5281/zenodo.5973788.

2.1. Species of interest – focus on dispersal, metapopulations and Allee effect

The two shad species share similar life-history strategies and ranges

Fig. 1. Conceptual diagram of the HyDiaD model starting with the modeling of habitat suitability followed by the insertion of population dynamical processes. At each time step t and for each catchment i, the two separate outputs are converted into number of fish and compared. The lowest value is retained as an estimation of the number of fish surviving maturity at time t for catchment i ($N_{i,t}$) (see Eq. (3)).

in the North-Eastern Atlantic (Wilson and Veneranta, 2019). The historic range of these species on the Atlantic coast extended from Norway to Morocco, though *A. fallax* has been reported as far north as Iceland (ICES, 2015). Both species are anadromous and migrate into freshwater to spawn in the spring (McDowall, 1988). Shad populations, especially those of *A. alosa,* have declined severely across Europe over the past century (Aprahamian et al., 2003; Baglinière et al., 2003; Nachón et al., 2016) due to a multitude of impacts along their migration routes acting at all life stages (Costa-Dias et al., 2009; Limburg and Waldman, 2009). While these shad species have the ability to travel long distances (Martin et al., 2015), both species generally exhibit homing (i.e. the return of fish to their natal river (Aprahamian et al., 2003; Jolly et al., 2012; Martin et al., 2015; Davies et al., 2020)), though short-distance dispersal likely occurs between neighboring rivers with similar environmental conditions (Aprahamian et al., 2003; Jolly et al., 2012; Martin et al., 2015). These localized exchanges might result in metapopulation dynamics with some rivers acting as "sources" and other as "sinks" (Randon et al., 2017). Interestingly, Rougier et al. (2012) demonstrated for Allis shad a likely demographic Allee effect (depensation in fish stock productivity when the abundance of spawners is low) for the reference population in the core of its distribution range. These complex dynamical processes possibly at play for the two shad species are crucial to consider when simulating species spatial responses to climate change.

2.2. Correlative species distribution model (C-SDM)

C-SDM were built and run to relate both the physical characteristics and environmental predictor variables of river catchments to the recorded presences and absences of each species within the equivalent time period. C-SDM were then used for projecting habitat suitability (between 0 = not suitable to 1 = perfectly suitable) annually for each catchment from 1951 to 2100 for three GCMs and two RCP scenarios (4.5 and 8.5).

2.2.1. Presence/absence data

For both shad species, presence/absence data to calibrate the C-SDM were available from the EuroDiad 4.0 database (https://data.inrae.fr /dataset.xhtml?persistentId=doi:10.15454/IVVAIC; Barber-O'Malley et al. (2022)). This database stores information about the

presence/absence and functionality (i.e., reproductive capacity) of diadromous species populations in selected catchments in Europe, the Middle East, and North Africa from 1750 to present time (Béguer et al., 2007; Lassalle et al., 2008b; Lassalle and Rochard, 2009). EuroDiad 4.0 stores data for 350 catchments and three time periods, though the precision of information varies and not every species has information for each time period. This database underwent two validation processes by local experts from various organizations involved in fisheries sciences and environmental management. The 292 catchments with presence/absence data available represented all of the large ($> 50,000\,\mathrm{km}^2$, $N = 37$) and medium-sized ($>10,000\,\mathrm{km}^2$, $N = 48$) catchments present in Europe, the Middle East, and North Africa, as well as 207 small-sized catchments ($<10,000\,\mathrm{km}^2$) that were specifically chosen to prevent any geographical bias in the database (Lassalle and Rochard, 2009). However, this represents only a proportion of the small-size catchments that exist within the study area. For shads, calibration was performed using all catchments with available presence/absence data for each species ($N = 254$ and 243 for *A. alosa* and *A. fallax,* respectively). This included 37 large, 47 medium and 159 small-sized catchments for *A. fallax* and 37 large, 48 medium, and 169 small-sized catchments for *A. alosa*. Projection of future distributions was focused on the same catchments for both species ($N = 135$) located in the Atlantic Area corresponding to their core distribution range and potential northern territories where the species distribution may shift under warming conditions.

2.2.2. Environmental predictor variables

Environmental variables used in C-SDMs were chosen to balance data availability with the potential to affect diadromous species distribution across Multiple species (Bradie and Leung, 2017). As these species utilize both freshwater and marine habitats, both continental and marine environmental variables were used for the first time to predict species distributions (Table 1). Continental variables included elevation at the headwater, length of the main watercourse, surface area of the drainage basin, and precipitation (see Lassalle et al. (2008) for their ecological meaning). The first three variables were provided for each catchment by EuroDiad 4.0. Precipitation was calculated as an annual value across the surface area of each catchment. These values represent the physical aspect of each catchment, and taken together can represent the range of hydrologic conditions that diadromous species experience

Table 1

Marine and continental environmental predictor variables used in the calibration of the correlative species distribution models for shads and the observed data sources used for describing the past.

Category	Environmental predictor	Source	Time Range	Type
Marine	Sea surface temperature	CHORE-AS	1901–2010	*Re-analysis*
	Surface salinity	CHORE-AS	1901–2010	*Re-analysis*
	Mixed layer depth	CHORE-AS	1901–2010	*Re-analysis*
Continental Catchment	Precipitation	CRU	1901–2018	Observed
	Surface area of the catchment	EuroDiad 4.0		
	Length of the main watercourse	EuroDiad 4.0		
	Altitude at the source	EuroDiad 4.0		

(Pont et al., 2005; Lassalle and Rochard, 2009). Marine variables at the outlet included surface salinity, sea surface temperature (SST), and mixed layer depth. While salinity and temperature are known to have direct physiological effects on anadromous fish, the mixed layer depth relates to the euphotic zone and biological production that might be of relevance for pelagic species (Bruge et al., 2016; Erauskin-Extramiana et al., 2019). Marine variables were calculated for each catchment using a buffer (of 0.5° side) around the outlet of the river to take into account the dilution of the river plume.

Observed atmospheric data came from the Climate Research Unit time-series dataset (CRU T.S. 4.03; crudata.uea.ac.uk) (Mitchell and Jones, 2005), which includes monthly climate observations measured at meteorological stations throughout Europe and interpolated between stations with a resolution of 0.5° (~ 62 km) from 1901 to 2018. Observed data for the marine variables came from the CHORE_AS (CMCC Historical Ocean Reanalysis) dataset, which is a reanalysis performed by the CMCC (Centro Euro-Mediterraneosui Cambiamenti Climatici; http://c-glors.cmcc.it/) (Yang et al., 2017) reconstructing ocean variables from 1900 to 2010 at a resolution of 0.5° degree (Table 1).

When using climate projections it is important to include the projections from multiple Global Climate Models (GCMs) in order to account for possible discrepancies between model estimates (Harris et al., 2014), in the kind of strategy commonly known as the use of ensembles. For marine environmental variables, we have used data from three different Global Climate Models (GCMs) that are detailed in Table 2 with trends presented in Fig. 2 for RCP scenario 8.5 and in Appendix C Figure C1 for RCP scenario 4.5. For atmospheric variables we have used data from three models from the EURO—CORDEX project (http://www.euro-cordex.net/), where several GCMs have been dynamically downscaled to achieve better spatial resolution and better representation of local atmospheric processes – these three Regional Climate Models (RCMS) (Table 3; Fig. 2, Appendix C Figure C1) and use the same GCMs as the ones used as marine data source to achieve minimally consistent grids. Climate projections were provided from 1951 to 2100, and as a suggested best practice ecological studies by Harris et al. (2014), two

Table 2

Global Climate Models used in this study.

Model	Center	Country	Reference
cnrm-cm5	Center national de recherches meterologiques (CNRM)	France	(Voldoire et al., 2013)
CSIRO–Mk3–6–0	Commonwealth Scientific and Industrial Research Organisation (CSIRO)	Australia	(Phipps et al., 2011, 2012)
NorESM1-ME	Norwegian Climate Center	Norway	(Bentsen et al., 2013; Iversen et al., 2013)

emissions scenarios were used for each GCM (RCP 4.5 and RCP 8.5, Table 4) and RCP to encompass a range of uncertainty in the projected increase in global mean temperature and to compare mitigated vs unmitigated responses. A correction procedure based in a quantile-quantile correction was also applied to each climate model to correct errors intrinsic to the model between a historical projection of modeled data from 1950 to 2005 and the observed data (the CHORE_AS reanalysis for marine variables and the ERA5 reanalysis for atmospheric variables) (Kotlarski et al., 2014; Casanueva et al., 2016). In this way of correcting data, it is assumed that there should be similar distributions of values between observed data, which represented reality, and the historical modeled projections, and any necessary corrections to ensure this similarity is propagated forward to the projections from 2006 to 2100.

2.2.3. Algorithm choice for habitat suitability models

Boosted regression trees (BRTs) were chosen to produce quantitative measures of habitat suitability because they can handle different types of predictor variables and missing values (De'ath, 2007). BRTs combine multiple, simple decision trees to optimize a model's predictive performance (Elith et al., 2008). Boosting involves growing a large group of trees in sequence and combining the averaged predictions (De'ath, 2007). The predictive error of this method is improved and over-learning is reduced using stochastic gradient boosting, which uses least squares regression trees and subsamples the training data to include randomness (Friedman, 2001; De'ath, 2007). Due to the limited data set, subsampling was accomplished through a cross-validation method with smaller datasets (De'ath, 2007). Subsets were formed using prevalence stratification to prevent overinflating the influence of absence data (Elith et al., 2008). Boosted regression trees were run in R language (R v. 4.0.3; R Core Team (2020)) using the "gbm" package (Greenwell et al., 2020).
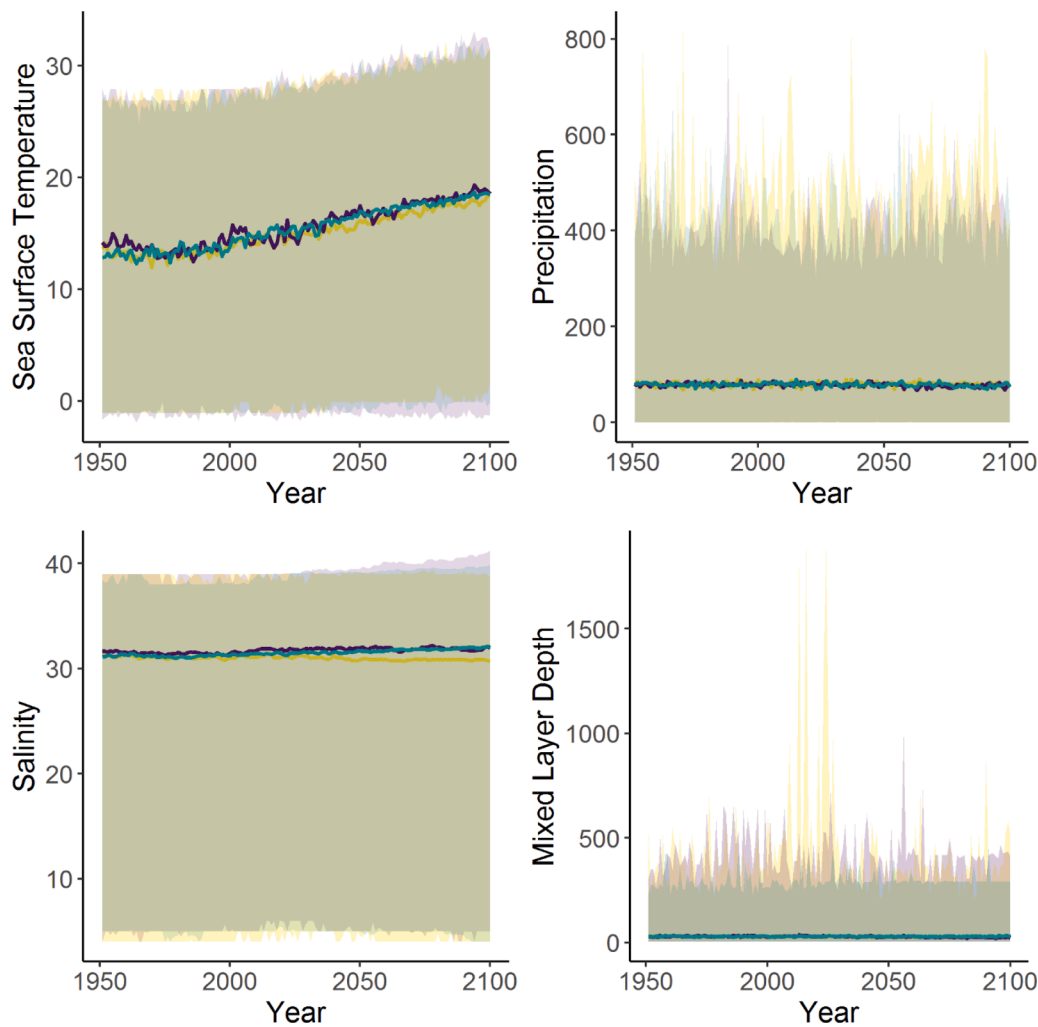
2.2.4. Model calibration procedure

As the model used presence/absence data, a Bernoulli classification for binomial data was used. Three metaparameters of the BRTs were adjusted for each species in order to optimize the predictive performance: bag fraction, the number of folds, and the learning rate (Table 5). The first two metaparameters relate to the cross-validation process internal to the model-building procedure. Model metaparameters were optimized for each species separately, and were adjusted so that the models converged and more than 1000 trees were produced, as suggested by Elith et al. (2008). The bag fraction determines the proportion of training versus testing data within each subset. This value was set at 0.7 to follow the convention of 70% of the data used for training and 30% for testing (Elith et al., 2008). The number of folds determines the number of random subsets to use for cross-validation. Here the common value of 10 was used. The learning rate determines the contribution of each tree to the model, and was optimized at 0.005 for both species. A smaller value for learning rate can reduce potential overfitting, but a larger value results in more trees which can improve the estimate of prediction error (De'ath, 2007; Elith et al., 2008). One additional parameter is tree complexity, which determines the number of splits in each tree. For both species, tree complexity was set to 1, meaning that only main effects were taken into account (Table 5).

After optimized metaparameters were determined, a test was run to see if the BRT model for each species could be simplified by dropping environmental predictor variables (Elith et al., 2010; Segurado et al., 2015). This is done by running a series of species-specific Jackknife tests that exclude each predictor variable sequentially, except for the two variables with the highest relative influence (Elith et al., 2011). A variable was dropped from the model if this test resulted in a decrease in the predictive deviance.

2.2.5. Tests of model accuracy

Several indices were then used to test model accuracy in reproducing the historic distribution for each species using the optimized

Fig. 2. Trends in projected marine and atmospheric variables from 1951 to 2100 under RCP 8.5. Marine variables (sea surface temperature, salinity, and mixed layer depth) are projected from three GCMs (yellow = CNRM-CM5, purple = CSIRO-Mk3–6–0, and blue = NorESM1-ME). Precipitation is projected from RCM RCA4 with driving models of yellow = CNRM-CM5, purple = CSIRO-Mk3–6–0, and blue = NorESM1-ME. (For interpretation of the references to colour in this figure legend, the reader is referred to the web version of this article.)

Table 3
Regional Climate Models (RCMs) used in this study.

RCM Name	Center	Resolution	Driving Model	Reference
RCA4	Swedish Meteorological and Hydrological Institute	0.44°	CNRM-CM5	(Jacob et al., 2014; Kotlarski et al., 2014)
RCA4	Swedish Meteorological and Hydrological Institute	0.44°	CSIRO–Mk3–6–0	(Jacob et al., 2014; Kotlarski et al., 2014)
RCA4	Swedish Meteorological and Hydrological Institute	0.44°	NorESM1-M	(Jacob et al., 2014; Kotlarski et al., 2014)

Table 4
RCP scenarios used in this study. Global mean temperature listed is for 2100 relative to 1900. European land temperature is for 2071–2100 compared to 1971–2000.

RCP	CO_2 Equivalent Concentration	Projected increase in global mean temperature[*]	Predicted increase in mean European land temperature[‡]	Climate policy
4.5	650 ppm	1.0–2.6 °C	1.4–4.3 °C	Mitigation in all countries
8.5	1350 ppm	2.6–4.8 °C	2.7–6.2 °C	No mitigation

[*] Harris et al. (2014).
[‡] Jacob et al. (2014).

Table 5
Optimized metaparameters for each shad species used for model projections with boosted regression trees.

Species	Family	# Trees	Tree Complexity	Learning Rate	Bag Fraction	# folds
A. alosa	Bernoulli	3250	1	0.005	0.7	10
A. fallax	Bernoulli	2500	1	0.005	0.7	10

metaparameters (Table 5). For threshold-dependent indices, including sensitivity, specificity, and TSS, fitted values from the boosted regression trees (or the estimates of habitat suitability comprised between 0 and 1) had to be converted to presence/absence values for evaluation. The threshold value used to define presence (above the threshold) versus absence (below the threshold) was estimated using the "evaluate" function in the package "dismo" (Hijmans et al., 2021). A confusion matrix of true and false presences and absences was used to calculate sensitivity, specificity, and the True Skill Statistic (TSS) for each species (Allouche et al., 2006). The TSS index measures the accuracy of each

Table 6

Indices of predictive accuracy used to evaluate boosted regression trees. n indicates the total number of presences and absences in the dataset.

Index	Formula	Description
True Presence	a	Number of observed presences correctly modeled as present
False Presence	b	Number of observed absences incorrectly predicted as present
False Absence	c	Number of observed presences incorrectly predicted as absent
True Absence	d	Number of observed absences correctly modeled as absent
Prediction Error	$1 - \dfrac{a+d}{n}$	Rate of incorrectly classified modeled values
Sensitivity	$\dfrac{a}{a+c}$	Proportion of correct classifications of presence (omission errors)
Specificity	$\dfrac{d}{d+b}$	Proportion of correct classification of absence (commission errors)
TSS[*]	Sensitivity + Specificity -1	True Skill Statistic: Accuracy of modeled data to what could have occurred by chance
AUC[‡]	Area under the receiver operating curve (ROC)	Threshold-independent measure of accuracy

[*] Allouche et al. (2006).
[‡] Fielding and Bell (1997).

calibrated model by comparing the model accuracy to how well the model performs by chance. This index can range from -1 to $+1$, with a value above 0 indicating that the model is performing better than random and a value of $+1$ indicating perfect accuracy. Threshold-dependent metrics can be interpreted according to the classification of Landis et al. (1977) (Table 7).

A threshold-independent measure of model accuracy was also estimated for both species. This was the AUC, which estimates the area under the receiver operating characteristic (ROC) curve. This method calculates the sensitivity and specificity for every possible threshold value between 0 and 1. The ROC curve plots sensitivity against the probability of incorrectly classifying a presence, or 1-sensitivity (Fielding and Bell, 1997) . Using the "gbm" package in R (Greenwell et al., 2020), the AUC score was calculated for each subset of data used for cross-validation ($k = 10$). The standard error of the AUC was also calculated for these subsets. An AUC value of 0.5 or lower indicates a classification no better than random, while a value of 1 indicates all modeled predictions were correctly classified (Swets, 1988).

2.3. Population dynamics and dispersal

The second component to the HyDiaD model built was coupled with the C-SDM by applying ad-hoc population and dispersal dynamics to estimate the number of fish produced in a given catchment i at time t. Population dynamics included an estimate of population growth rate (r) and an Allee effect (λ) (Table 8). Within the HyDiaD model, the Allee parameter was related to the number of spawners that participated in reproduction within a given catchment. A high value for the Allee

Table 7

Ranking value and interpretation according to Landis et al. (1977) for threshold-dependent metrics.

TSS value	Interpretation
< 0	no agreement
0 to 0.2	slight
0.2 to 0.4	fair
0.4 to 0.6	moderate
0.6 to 0.8	substantial
0.8 to 1	perfect

parameter reduced the proportion of spawners that participated in reproduction, making it difficult for populations to persist at a low abundance. This also affects the settlement of a population in a novel catchment, as a minimum number of spawners need to be present in a given year for reproduction to exceed the limitation imposed by the Allee effect. This parameter interacted with the population growth rate in that a high value for the latter could reduce the effect of the former. Dispersal dynamics included an estimate of the probability of emigration (γ), an additional mortality rate associated with emigration (M_{disp}), and a measure that incorporated both the long and short-distance dispersal capabilities of a species (α and β used to estimate a dispersal kernel).

2.3.1. Simulating different age classes

Within the HyDiaD model, both the habitat suitability and estimate of spawner abundance are calculated on an annual time step. The model was developed to simulate a temporal lag between the production of a cohort of fish in a given year and when those fish enter the spawning population and contribute to future production. This time lag can be defined based on the life history parameters of the species using the average age at maturation (m_a). In addition, while the spawning population within a given year is not explicitly age-structured, the model is capable of utilizing multiple spawner age classes to estimate $N_{i,t}$ in a given time step using a parameter for the number of cohorts (n_c). When n_c is set to 1, there is no age structuring in the estimation of $N_{i,t}$ for the current time step, and only a single year contributes to the current production. A value of n_c for $i > 1$ simulates a population with multiple cohorts that contribute equally to production in the current year. The term n_c is used to define the set (S) of ages S_k at which fish contribute to spawning and production in year t such that:

$$S = \{S_k\}_{k=1}^{n_c} \tag{1}$$

When both a temporal lag and age structure are simulated in the model, m_a defines the average of all items in set S, and n_c defines the spread around that number as follows:

$$S_k = \left\lfloor m_a + k - \frac{n_c}{2} \right\rfloor \tag{2}$$

Of the set S, s_1 is the minimum generation time, and will always be ≥ 1 year. The item S_{n_c} will be the maximum generation time, and will always be $\leq 2 * m_a$

2.3.2. Initial habitat suitability

Calibration of C-SDMs was performed using observed historical data to estimate "initial" habitat suitability within each catchment i ($HSI_{i, t = 0}$) representing conditions at the beginning of the model run, which was then used to calculate initial spawner abundance ($N_{i, t = 0}$) as follows:

$$N_{i,t=0} = HSI_{i,t=0} * D_{max} * A_i \tag{3}$$

where D_{max} was a species-specific estimate of the maximum density of spawners in ideal conditions and A_i was the surface area of catchment i. It was assumed that these initial values represented a system in equilibrium (Hanski, 1994; Singer et al., 2018). Initial habitat suitability was estimated for each catchment using observed data for environmental predictors (CRU and CHORE-AS) averaged from 1901 to 1911 and presence/absence data (EuroDiad 4.0) from the period 1851–1950. This time period was chosen to represent species distributions right before what is called the "Great Acceleration" in human activities during the Anthropocene (Steffen et al., 2015), but was also a compromise with environmental data availability. This initial value of habitat suitability, along with population and dispersal dynamics described in the next section, were used for a burn-in period of 50 years, i.e. outputs were discarded. After the burn-in period, annual predictions of habitat suitability from 1951 to 2100 were estimated using modeled projections of the same environmental predictor variables averaged across multiple GCMs and RCP scenarios (as described below).

Table 8

Parameters in the population dynamics component of the HyDiaD model with values for *A. alosa* and *A. fallax*. Weighted estimates for some expert knowledge survey parameters (indicated in italics) were calculated on a log scale. For these logged parameters, the three values listed indicate the weighted mean, lower standard error (SE), and upper SE, respectively. For parameters that were not logged, the SE is indicated following "±".

Parameter	Description	Unit	Range	Source	*A. alosa*	*A. fallax*
D_{max}	Maximum density of fish in ideal conditions	fish km^{-2}	[0, +∞]	Expert knowledge survey	*7.107, 4, 10*	*4.068, 2, 8*
γ	Probability of emigration	–	[0, 1]	Expert knowledge survey	0.163 ± 0.11	0.131 ± 0.10
M_{disp}	Mortality rate for emigrants during dispersal	km^{-1}	[0, +∞]	Expert knowledge survey	0.54 ± 0.33	0.58 ± 0.35
α	Scale parameter for the dispersal kernel (negative exponential)	km^{-1}	[0, +∞]	Calibrated using results from expert knowledge survey	0.444	0.547
β	Shape parameter for the dispersal kernel (negative exponential)	–	[0, +∞]	Calibrated using results from expert knowledge survey	0.417	0.418
r	Population growth rate	–	[0, +∞]	Expert knowledge survey; (Whitehead, 1985; Quignard and Douchement, 1991)	2.13	3.05
λ	Parameter for the Allee effect	–	[0, 1]	Expert knowledge survey	*0.093, 0.03, 0.3*	*0.442, 0.02, 1*
m_a	Average age of maturity	year	[0, +∞]	(ICES, 2015)	5	5
n_c	Defines the number of cohorts to include in spawner production in the current time step t	–	[0, +∞]	(Kottelat and Freyhof, 2007)	3	3
A_i	Surface area of catchment i	km^2	[0, +∞]	EuroDiad 4.0		
d_{j-i}	Distance between catchments j and i	km		EuroDiad 4.0		
$HSI_{i,t}$	Habitat suitability index of catchment i in time t	–	[0,1]	BRT model output		
$N_{i,t}$	Number of fish that survive to maturity in catchment i in time t	individual	[0, +∞]	Hybrid model output		
$B_{i,t}$	Total of spawners that return to catchment i as their origin catchment and spawners that disperse to catchment i from all surrounding catchments	individual	[0, +∞]	Hybrid model output		
h_1	Anthropogenic effects related to habitat degradation		[0, +∞]	NA	0	0
h_2	Anthropogenic effects related to direct mortality		[0, +∞]	NA	0	0

2.3.3. Population dynamics and dispersal process

Spawner abundance in time t ($B_{i,t}$) was estimated as the sum of spawners N returning to their origin catchment (i) on the left side of Eq. (4) and spawners dispersing into catchment i from surrounding catchments on the right side of the same equation:

$$B_{i,t} = \left(\left[S \sum \frac{N_{i,t-S}}{n_c} * (1-\gamma) \right] + \sum_{j \neq i \in \Omega} \left[S \sum \frac{\frac{N_{j,t-S}}{n_c} * \gamma * e^{-\alpha d_{j-i}^{\beta}}}{\sum_{l \neq j \in \Omega} e^{-\alpha d_{j-l}^{\beta}}} * e^{-M_{disp} d_{j-i}} \right] \right) * e^{-h_2}$$

(4)

where γ is the probability of emigration, M_{disp} is the mortality rate for emigrants during dispersal, and h_2 is an anthropogenic source of mortality (e.g. from a fishery). These three parameters are species-specific, but are considered as a constant across all catchments and through time. M_{disp} is an additional mortality coefficient that is only applied to emigrants entering a surrounding catchment different from their natal catchment. This mortality rate is applied according to the distance between natal and destination catchments ($d_{i,j}$).

An extended negative exponential kernel function (De Cáceres and Brotons, 2012) was used to determine the number of spawners arriving in catchment i from each catchment j in the set of possible catchments Ω. This kernel function ($e^{-\alpha d_{j-l}^{\beta}}$) is calculated using the distance between catchments i and j (d_{j-i}), and incorporates both long and short-distance dispersal through the scale parameter α and the shape parameter β (Chapman et al., 2007). Distance between each pair of catchments was calculated as the shortest path following the coastline between the outlets of each catchment. This corresponded to the sum of the shortest paths from the departure catchment outlet to the coastline, from the destination catchment outlet to the coastline, and between the two corresponding points on the coastline. However, the distance between a

catchment and itself was fixed to 0 regardless of the position of the outlet in relation to the coast line.

The central calculation in HyDiaD is the number of fish that survive to maturity in catchment i at time t ($N_{i,t}$). It was estimated by taking the minimum of the two values coming from the two model components, i.e. the habitat suitability model on one side and the ecological dynamics on the other side using the following equation:

$$N_{i,t} = min\left[HSI_{i,t} * D_{max} * A_i * e^{-h_1}, B_{i,t} * r \right],$$

(5)

where $HSI_{i,t}$ is the habitat suitability index for catchment i at time t, D_{max} is the maximum density of fish per km^2 for a given species, A_i is the surface area of catchment i, h_1 is a measure of anthropogenic effects related to habitat degradation, $B_{i,t}$ combines spawners that return to their origin catchment and spawners that disperse into catchment i from surrounding catchments as defined in Eq. (4), and r is a constant growth rate applied to all catchments. Defining $N_{i,t}$ as the minimum of the two separate components in this equation simulates a hockey-stick recruitment curve (Barrowman and Myers, 2000). The population grows at a rate r until it reaches a limit set by the habitat suitability at time t that is specific for that species (D_{max}) and catchment (A_i).

Eq. (3) was then modified to include an Allee effect as follows:

$$N_{i,t} = min\left[HSI_{i,t} * D_{max} * A_i * e^{-h_1}, B_{i,t} * \frac{B_{i,t}^2}{B_{i,t}^2 + (\lambda * D_{max} * A_i)^2} * r \right]$$

(6)

In this equation, $B_{i,t}^2 / (B_{i,t}^2 + (\lambda * D_{max} * A_i)^2)$ indicates the proportion of spawners that are participating in reproduction. This means that 50% of spawners participate when $B_{i,t} = \lambda * D_{max} * A_i$.

2.3.4. Collecting model parameters for shads and modeling postulates

The HyDiaD model was parameterized for the two shad species using parameter values listed in Table 8 and run on a yearly time step from 1951 to 2100. The framework was developed to include two types of

anthropogenic influences (h_1 and h_2). Current information related to habitat accessibility is available for larger European rivers (https://www.eea.europa.eu/; Lassalle et al. (2010)); however, historical data was needed for the calibration of the C-SDM and this was not available for many of the catchments included. Though the authors considered several proxies for anthropogenic influences, such as human population density (Lassalle et al., 2010) and Gross Domestic Product. Nevertheless, it was difficult to find historical data that covered the spatial extent of the European Atlantic area, but also had a fine enough resolution to estimate differences on a catchment-to-catchment scale. A coarse spatial resolution would not allow the C-SDM to differentiate between conditions that result in a presence versus an absence, meaning the model would not be able to "learn" the relationship between anthropogenic influences and occupancy (Elith et al., 2008). Thus, it was not possible to include anthropogenic influences as parameters h_1 and h_2 within the scope of the current study for shads. While no local anthropogenic pressures (i.e. h_1 and h_2 set to 0) were included for shads, general anthropogenic pressures such as climate-induced changes were included in the form of abiotic environmental predictor variables as described above. This implied that spawner abundance estimates in HyDiaD represented a "maximum potential". So, by using HyDiaD to make simulations, the postulate was made that the underlying assumptions of the model remained all suitable for the actual and future system.

Species-specific parameter values for the population and dispersal dynamics in the HyDiaD model, as well as an estimate of maximum density of spawners in ideal conditions needed to convert HSI into spawner abundance, were estimated using the primary literature or through the solicitation of knowledge from diadromous species experts (Table 8). The latter was accomplished using a 10-question, iterative online expert knowledge survey that was specifically developed to estimate values for population demographics using a Delphi process, which is used to address scientific questions with high levels of uncertainty that are difficult to empirically measure (Elmer et al., 2010). While this questioning technique has been used in a variety of ways, the basic components include soliciting expert knowledge using a standardized questionnaire through several rounds of survey to estimate a group answer (Elmer et al., 2010). The expert knowledge survey in the current study was performed in two rounds (See Appendix A for more details). For the first round, each participant was provided the same written questions and was asked to complete the survey individually (See Appendix A). Group results were calculated and presented to participants during a workshop, and then a second round was completed using one-on-one interviews via video conferencing. This allowed participants to consider their answers in a group context, the authors to receive feedback on the process, and a more in-depth discussion to ensure that questions were being interpreted in the same way by all participants. The survey combined expert knowledge regarding species populations in multiple countries in order to estimate parameter values that represented this large spatial scale. As part of the expert knowledge survey, participants were asked to provide an estimate of their level of confidence in their response to use as a weighted measure. For each survey question, the group average and variance was calculated using weighted individual responses, as described in Appendix A. The final group averages calculated for use in the hybrid models used responses and confidence levels from this second round of the expert knowledge survey with a confidence level for each question and species combination.

2.4. Sensitivity analysis on HyDiaD parameters

A global sensitivity analysis was conducted to determine which parameters had the largest effect on the estimate of total spawner abundance summed across all catchments and years ($\sum N_{i,t}$) for each shad species in order to explore the relative influence of habitat suitability and population and dispersal dynamics. This analysis used the package "sensitivity" in R (Iooss et al., 2021), and utilized the Morris's

Elementary Effects (EE) screening method with a One At a Time (OAT) approach (Morris, 1991). This screening method utilizes a design that consists of multiple individual trajectories that move through the parameter space varying one factor (X_i) k times (equal to the number of parameters) along a grid with size Δ_i while keeping all the other factors fixed (Campolongo et al., 2007). Each trajectory results in one calculation of the Elementary Effect for the ith parameter, as shown in the following equation (Morris, 1991):

$$EE_i = \frac{Y(X_1, ..., X_{i-1}, X_i + \Delta_i, X_{i+1}, ..., X_k) - Y(X_1, ..., X_p)}{\Delta_i} \tag{7}$$

In order to account for interactions, multiple trajectories (r) were performed, each starting from a randomly sampled point. The set of EE from r trajectories are averaged to get an estimate of total-order sensitivity. In order to prevent EE_i with opposite signs from cancelling each other, an average (μ_i^*) was estimated using the absolute values of EE_i as suggested by Campolongo et al. (2007). In order to explore interactions and non-linear effects, the standard deviation (σ_i) of EE_i was also calculated. Plotting the results for μ_i^* against σ_i indicated which factors had negligible effects (both have low values), linear and additive effects (μ_i^* is high but σ_i is low), and nonlinear effects or interactions (both have high values).

The sensitivity analyses for the two shad species involved varying the seven parameters estimated from the expert knowledge survey (Table 8). The range of possible values for each parameter was determined by the upper and lower standard errors calculated for each shad species from the expert knowledge survey. For each parameter, this possible range of values is sampled evenly by defining a value for p (generally 4, 6, or 8), which corresponds to a percentile (25th, 17th, and 12.5^{th}, respectively) of the uniform distribution for each parameter (Morris, 1991; Campolongo et al., 2007; Franczyk, 2019). For both shad species, p was defined as 6 and a total of 20 trajectories (r) were used in the design to calculate (μ_i^*).

2.5. Saturation rate to compare results among catchments and species and to evaluate the added value of a hybrid approach

The output of the HyDiaD model is spawner abundance, but the primary intention of developing this modeling framework is to investigate variability in climate-induced spatial and temporal trends for multiple diadromous species within the same range of catchments. In addition to the habitat suitability (between 0 and 1) and spawner density (number of spawners per km²), an index was developed to facilitate comparisons across different-sized catchments and among different species, termed the saturation rate (SR). This is calculated for each catchment i at time t as follows:

$$SR_{i,t} = \frac{N_{i,t}}{HSI_{i,t} * D_{max} * A_i} \tag{8}$$

This index has a value between 0 and 1, and is limited by the HSI of a particular catchment in time t. A value close to 1 indicates that the abundance of the population is close to its maximum as defined by the habitat suitability. A value close to 0 indicates that the population abundance is much smaller than it could be. Therefore, the saturation rate informs on the interest to run a hybrid model compared to a strictly correlative approach. A low SR value indicates the high contribution of dispersal and demography in the population dynamics and thus the added value of considering a more complex approach when modeling a species distribution.

The HyDiaD model was run for each shad species from 1951 to 2100, and $N_{i,t}$ was calculated annually for all catchments in the Atlantic Area. Annual spawner abundance was used to calculate annual saturation rate. Results were presented as heat plots that were created in the package "ComplexHeatmap" in R (Gu et al., 2016) to compare trends through time in saturation rate, spawner density, and habitat suitability

among catchments. Individual catchments were included in heat plots as rows, and individual years as columns. Catchments were ordered by country in the plots, then arranged north to south within a region according to latitude. The annual spawner abundance averaged from 1951 to 1980 was also calculated in order to make general comparisons among individual catchments. For each species, heat plots were created by separately modeling the three GCMs, then averaging the results for each of the two RCP scenarios.

2.6. HyDiaD evaluation based on the saturation ratio metric

To further demonstrate the advantage of increasing the model complexity with a population dynamics and dispersal module, and to validate HyDiaD estimations with observations, two analyses were performed. First, the distribution of decadal SR values was inspected across all the catchments included in the HyDiaD physical environment. For a given year between 2041 and 2050, and a specific catchment, SR values were averaged across the three GCMs under the most pessimistic scenario RCP 8.5. Then, the decadal means from 2041 to 2050 were calculated and plotted together as a histogram. The skewness and spread of the distribution were examined to assess the relative contribution of the population dynamics and dispersal module compared to a strictly correlative approach. Secondly, observed abundances stored in EuroDiad 4.0 for the most recent period (i.e. 2010 - present times) were compared to the saturation ratios calculated on the maximum abundances (i.e. with an HSI of 1; $SR_{HSI=1}$) across the period 2010–2019. Abundances in EuroDiad are categorical with: (i) Absent (1) - the species was never recorded in the basin or was extirpated; Rare (2) - occasional vagrants were recorded in the basin; Common (3) - functional populations were present in the basin; and Abundant (4) - functional populations were present and numerically dominant in the freshwater community (Barber-O'Malley et al., 2022). For a given year between 2010 and 2019, and a specific catchment, $SR_{HSI=1}$ values were averaged across the three GCMs under the most pessimistic scenario RCP 8.5. Then, the decadal means from 2010 to 2019 were calculated for each catchment in the HyDiaD physical environment and categorized into four groups with one group for $SR_{HSI=1}$ equal to 0 and the three others being defined as equal range classes (with 1/3 and 2/3 as limits). A confusion matrix with these two categorical variables was built and the results analysed following the matrix diagonal that represents the records that are in agreement. Considering that HyDiaD is run without any anthropogenic impacts, estimates should be in the same categories or the ones above the observations of current abundances (i.e. on the diagonal or in the matrix lower half).

3. Results

3.1. C-GCM calibration and validation for shads

Tests related to habitat model simplification as part of the calibration process did not result in a decrease in predictive deviance for either shad species (Figure B2 in Appendix B), so all seven environmental predictor variables (Table 1) were used in the BRT model for predictions of habitat suitability. Prediction error was low for both shad species, but was lower for *A. alosa* than *A. fallax* (Table 9). The confusion matrix for *A. alosa* indicated roughly the same number of false presences and false absences, while *A. fallax* estimated a higher number of false presences than false absences (Table B1). Predictive accuracy was high for both species and all indices used (Table 9). Threshold-dependent indices were between 0.7–0.9, corresponding to "substantial" or "perfect" on the scale proposed by Landis et al. (1977) (Table 7). The threshold-independent AUC was above 0.8, indicating that model accuracy was better than random (Table 9; Figures B3 and B4).

The marine and continental environmental predictor variables with the highest relative influence differed slightly between the two shad species. For *A. alosa*, the top environmental predictors were mixed layer

Table 9
Measures of predictive accuracy of BRT models for the two shad species. CV AUC score was calculated using the subsets used for cross-validation. SE refers to standard error of these subsets. Prevalence is the proportion of presences in the observed data. Formulas for indices are given in Table 6.

Index	*A. alosa*	*A. fallax*
Prevalence	0.221	0.537
Threshold	0.37	0.49
CV AUC score	0.831	0.812
CV AUC SE	0.025	0.027
Prediction Error	0.075	0.116
Sensitivity (Omission)	0.821	0.938
Specificity (Commission)	0.954	0.821
TSS	0.776	0.760

depth, precipitation, and altitude (Fig. 3). The top environmental predictors for *A. fallax* included precipitation, sea surface temperature, and altitude (Fig. 4). Several of these predictor variables had steep response curves, meaning that a small change in the predictor variable could result in a relatively large change in habitat suitability.
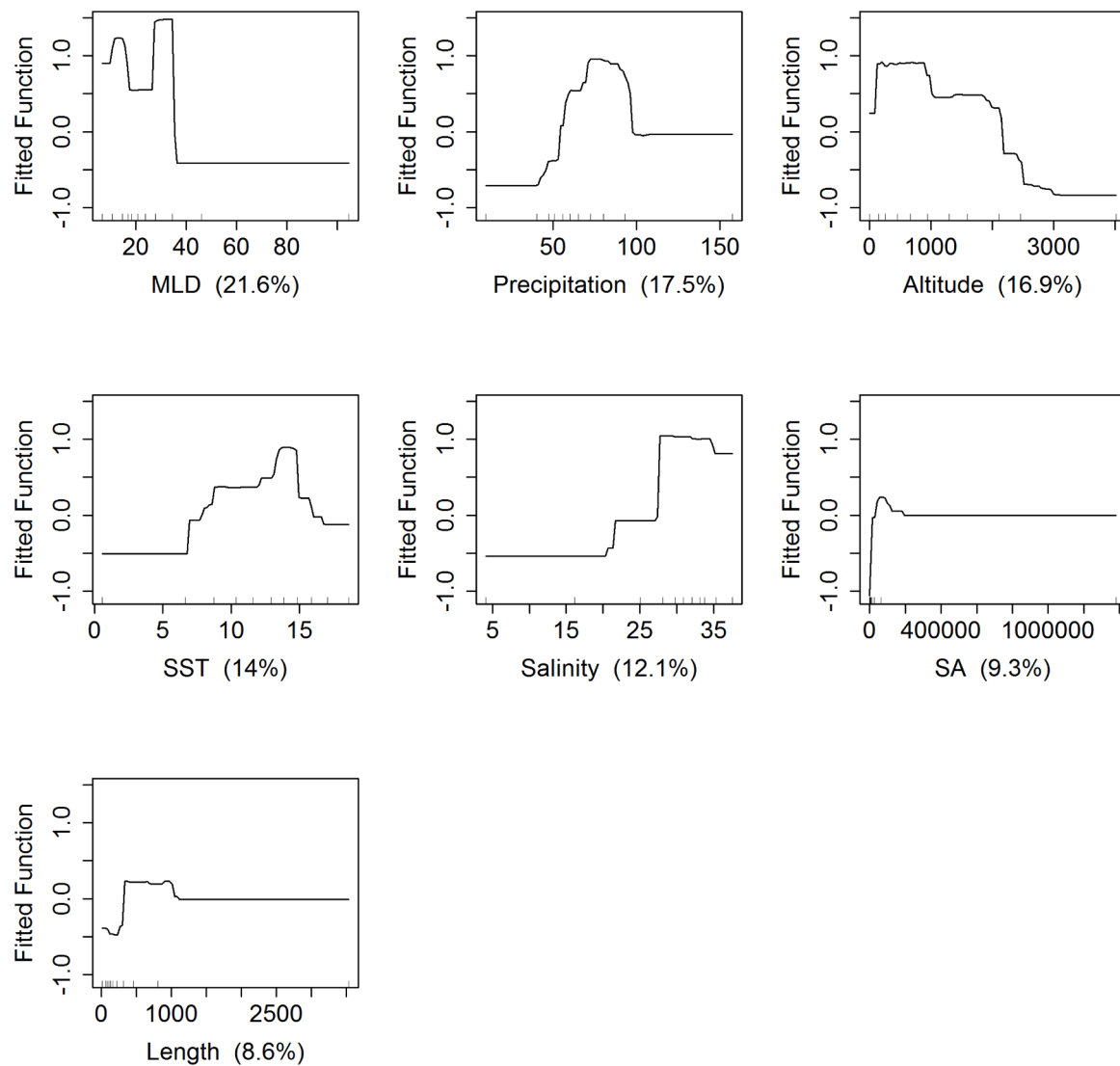
The estimate of habitat suitability was generally lower and displayed more annual variability for *A. alosa* than for *A. fallax* (Figs. 5 and 6). Response curves for *A. alosa* indicated a total relative contribution of 31.5% for annual continental precipitation and annual sea surface temperature. These two variables had a unimodal distribution with a decrease in habitat suitability for catchments with values at the two extremes of the range of possible values (Figs. 3 and 5). While response curves for *A. fallax* indicated a similar decrease in habitat suitability at the lower range of precipitation and sea surface temperature, with a total relative contribution of 41.5%, this species did not see a decrease in estimated habitat suitability as the predictor variables increased to their upper range (Figs. 4 and 6). In addition, *A. alosa* had a bimodal response curve for annual mixed layer depth, while *A. fallax* generally saw a decrease in habitat suitability as mixed layer depth increased. Taken together, this indicates that in general *A. alosa* had fewer instances where the value of certain predictor variables could result in a high estimate of habitat suitability.

3.2. Expert knowledge survey results

In total, 12 participants responded for *A. alosa* and 14 for *A. fallax* from five Atlantic Area countries (Figure A1). Not all the participants provided answers to each of the 10 questions, though all questions had at least seven responses that were used when calculating the weighted mean and variance (Table 8). Results for both shad species indicated relatively high agreement between participants for five of the seven questions used to estimate model parameters, as seen when considering the standard error values (Figures A2-A4). The two questions focused on emigration, addressing the proportion of the population that emigrates and the survival rate for these emigrants had the highest variability between individual responses (Figure A5). Of these two questions, the one estimating emigrant survival rate had the largest standard error. Weighted estimates derived from this expert knowledge survey were presented in Table 8.

3.3. Projections of climate change impacts on shad distribution using HyDiaD

General spatial and temporal trends in projections differed among catchments and between shad species. Four types of temporal trends were seen when results were averaged across the three GCMs, including populations that 1) started with a spawner density (number of spawners per km^2) that was very low or zero and maintained that density through time (ex: Fig. 5, Vefsna, Norway), 2) started at a low spawner density and increased through time (ex: Fig. 5, Elbe, Germany), 3) started at a medium to high spawner density and decreased (usually to zero)
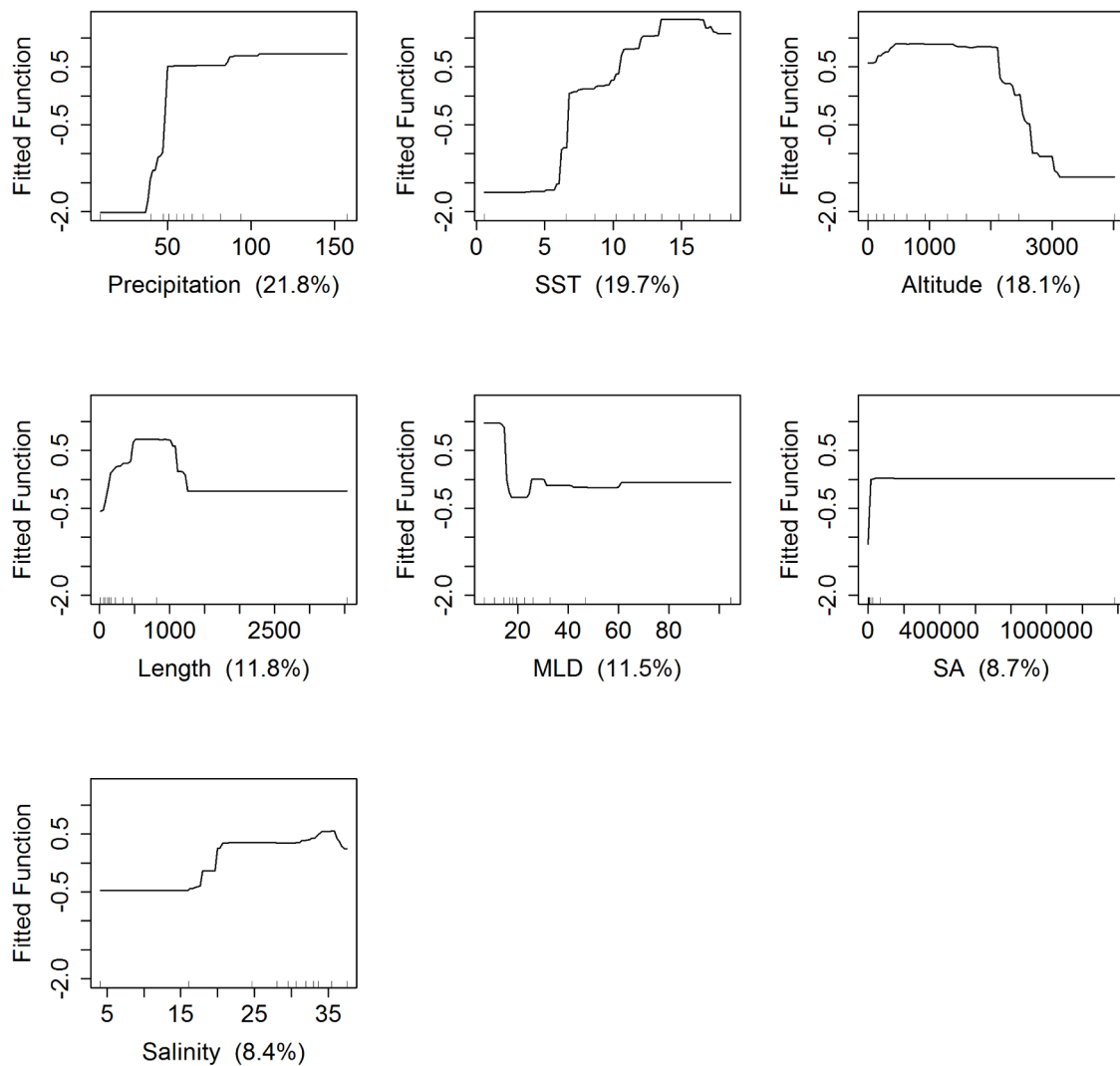
Fig. 3. Response curves for *A. alosa* for the seven environmental predictor variables selected by the calibration procedure (MLD: mixed layer depth, Altitude: altitude at the source; SST: sea surface temperature, SA: surface area of the catchment, Length: length of the main watercourse). Each panel shows the effect of one predictor variable on the fitted function after accounting for the average effects of all six of the other predictor variables. Variables are ordered by the value of their relative influence, as indicated by the percentage on the x-axis label, with the highest value shown in the top left panel.

through time (ex: Fig. 5, Adour, France), and 4) maintained a medium to high spawner density through time (ex: Figs. 5 and 6, Meuse, France). Using the dispersal parameters estimated through the expert knowledge survey, there were no instances where the population declined to near local extinction and then later increased again. For both species, instances where populations declined to zero (or "collapsed") corresponded to catchments with higher annual variability in HSI that often spanned the range of possible values. This is in contrast to populations that maintained a consistent spawner density through time, which had a relatively narrow range (i.e. 0.4 to 0.8) of annual HSI values projected from 1951 to 2100.

Large differences in averaged projected trends for habitat suitability and spawner density existed between the two shad species for the two RCP scenarios (Figs. 5 and 6). *A. alosa* generally demonstrated a more variable and consistently lower value for habitat suitability across all catchments (Fig. 5). While several individual catchments (from North to South, Weser, Ems, Meuse, Escaut, Seine, Loire, Charente, Dordogne, Garonne, Minho, and Mondego) had relatively high spawner density through time, the majority of catchments were consistently at the lower range of possible values. This is in contrast to *A. fallax*, which

demonstrated a spawner density at the higher range across the majority of catchments (Fig. 6). This trend was reflected in the projected HSI for *A. fallax*, which was high for most catchments except for several located in Spain, Portugal, and Morocco (e.g. Odiel, Tinto, Piedras, Sado, Mira, Loukkos, and Sebou). For this species, HSI was seen to increase through time for many catchments, especially in the northern extend of its range (above approximately 48°N). This temporal trend was less common for *A. alosa*, which often displayed high annual variability in HSI within a catchment. For *A. alosa*, some catchments did display an increase in HSI through time. However, the opposite was also true and several catchments saw a decrease in HSI through time. In addition, latitudinal trends in HSI were less clear for *A. alosa* than for *A. fallax*.

While spawner density and habitat suitability were both dramatically different between the two shad species as detailed above, trends in saturation rate were similar. For both species, the saturation rate was generally at one extreme or the other, representing either zero (a population crash) or 1 (the available habitat in that catchment is being fully utilized). However, some individual catchments did demonstrate annual variability in saturation rate (ex: Blavet in France and Guadiana in Spain, which both varied between 0 and 1 for *A. alosa*), which was seen
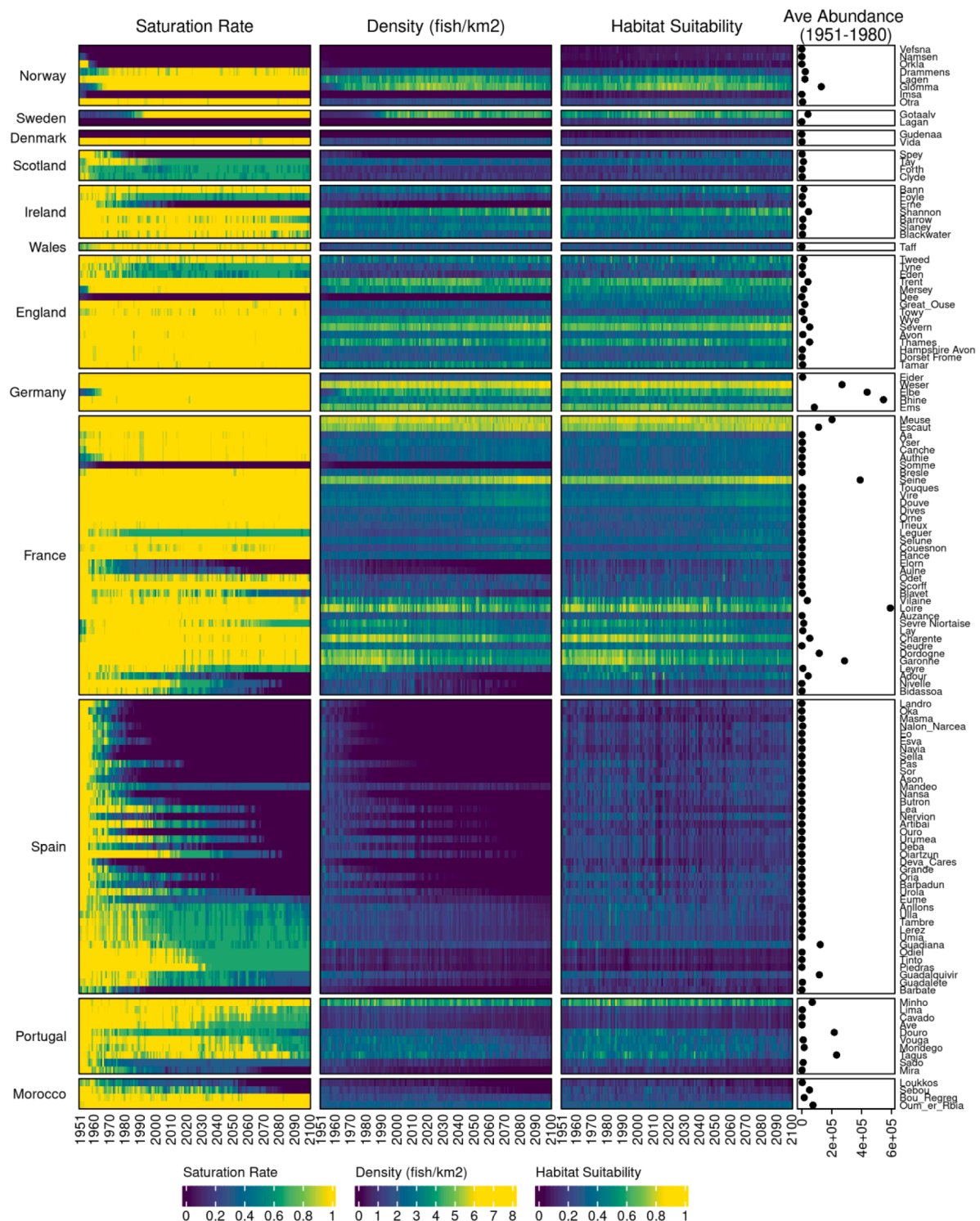
Fig. 4. Response curves for *A. fallax* for the seven environmental predictor variables selected by the calibration procedure (MLD: mixed layer depth, Altitude: altitude at the source; SST: sea surface temperature, SA: surface area of the catchment, Length: length of the main watercourse). Each panel shows the effect of one predictor variable on the fitted function after accounting for the average effects of all six of the other predictor variables. Variables are ordered by the value of their relative influence, as indicated by the percentage on the x-axis label, with the highest value shown in the top left panel.

more for *A. alosa* than *A. fallax*. It is important to keep in mind that saturation rate does not reflect the size of the population, but rather how the available habitat, though scarce, was being used by the population. A high saturation rate close to 1 could occur regardless of the value of habitat suitability. For both species, many catchments started with a high saturation rate that quickly decreased over a short period of time, as was demonstrated in Figs. 5 and 6 where the color rapidly shifted from yellow to dark blue. This trend could occur when the population started at a large abundance and rapidly collapsed, or when the habitat suitability and spawner density were relatively low in a catchment, but the population was still as large as it could be given the value of habitat suitability. When the value of habitat suitability was low, it limited the population growth. As could be seen for both species, once a population collapsed (saturation rate and density of 0), it did not later recover, as would be indicated by an increase in spawner density and saturation rate. These population collapses were much more prevalent for *A. alosa* (37%) than for *A. fallax* (10%) when considering the results from the three GCMs averaged together for RCP 8.5 (Figs. 5 and 6). The saturation ratio can also be defined as the comparison of the spawner abundances estimated by HyDiaD and the habitat model (C-SDM) alone. So, dominance of values close to 1 in the heat plots indicated no lag between changes in HSI values and the response of the population.

Model projections were similar between RCP 4.5 and RCP 8.5 for saturation rate, spawner density, and habitat suitability for both shad species (Figs. 5, 6, C2, and C3). The largest difference between the two scenarios related to the scale of change, which was seen in the temporal trends for habitat suitability. The amount of change that occurred between the earlier and later time series was more pronounced, as expected, for climate scenario RCP 8.5 than RCP 4.5. A good example of these differences can be seen for *A. alosa* in the Severn in England in Figs. 5 and C2. For RCP scenarios, HSI and spawner density are in the mid to high end of their range. Starting at roughly 2070, however, the values for both HSI and spawner density increase to consistently be higher for RCP 8.5 than RCP 4.5. However, when considering trends across all catchments, the difference in projected habitat suitability between the two RCP scenarios was negligible.

3.4. Sensitivity of total spawner abundance to model parameters

Results from the global sensitivity analysis were similar for the two shad species (Fig. 7). The parameters related to dispersal (i.e. mortality of emigrants (M_{disp}), the probability of emigration (γ), and the shape (β) and scale (α) parameters for the dispersal kernel; Table 8) had negligible effects on the total spawner abundance summed across all years and
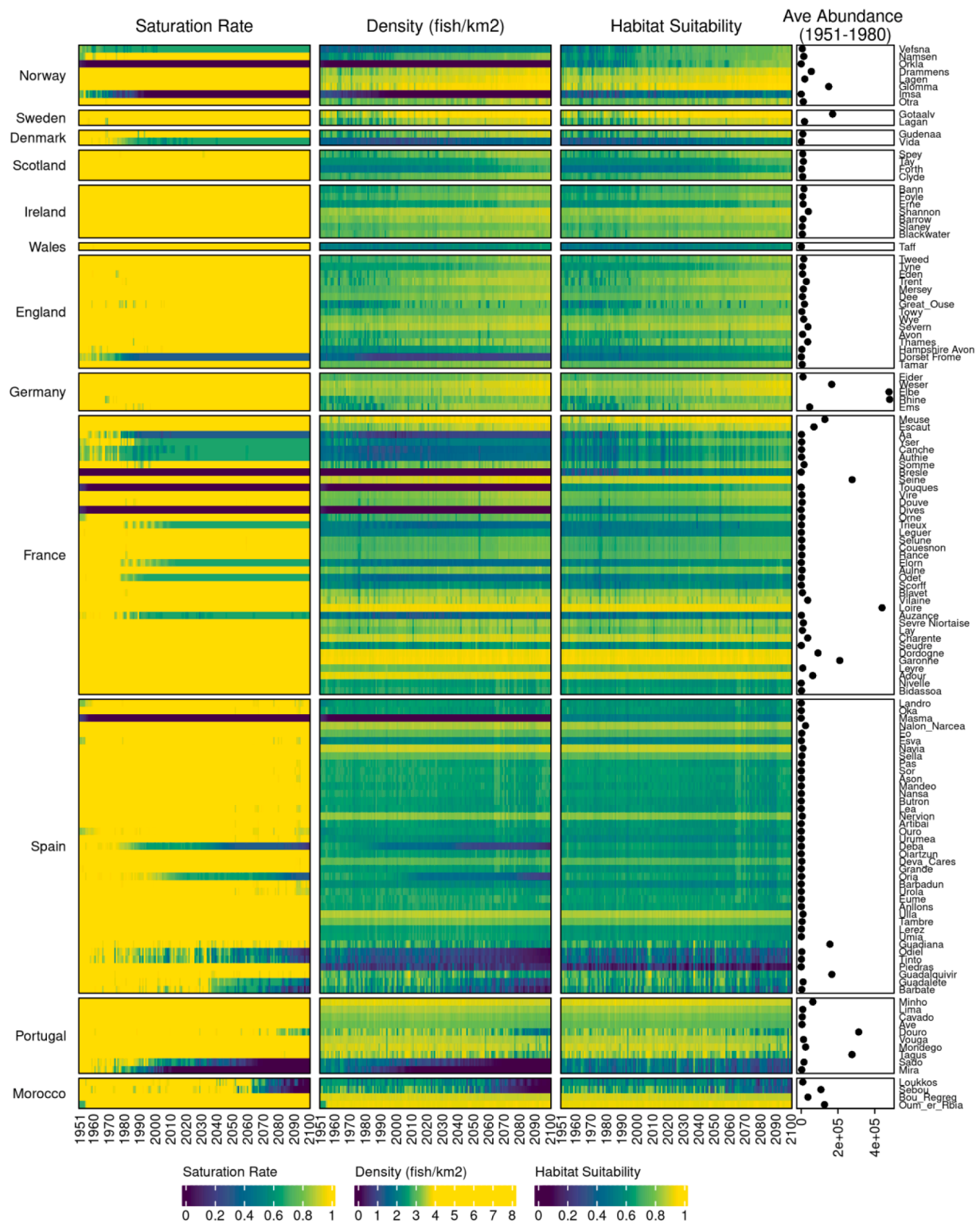
Fig. 5. Projections of saturation rate, spawner density and habitat suitability (HSI) averaged across three global climate models (GCMs) for *A. alosa* for different European catchments under climate scenario RCP 8.5 from 1951 to 2100. For heat plots, dark blue indicates smaller value and yellow indicates higher value. However, note difference in scale (indicated in legend) for the three heat plot panels. Fourth panel shows spawner abundance averaged for each catchment from 1951 to 1980 to provide a reference for a time horizon before populations started to change with climate change. Catchments are organized by country (indicated on left) and arranged within a country from north (top) to south. Individual catchment names are indicated on the right. See Appendix C for RCP4.5 results. (For interpretation of the references to colour in this figure legend, the reader is referred to the web version of this article.)

catchments as indicated by the low values of both σ and μ for all of these factors. The parameters related to population dynamics (i.e. population growth rate (r), the Allee effect (λ), and the maximum density of spawners per unit area (D_{max})) demonstrated a nonlinear effect or interaction because of a high value for both σ and μ.
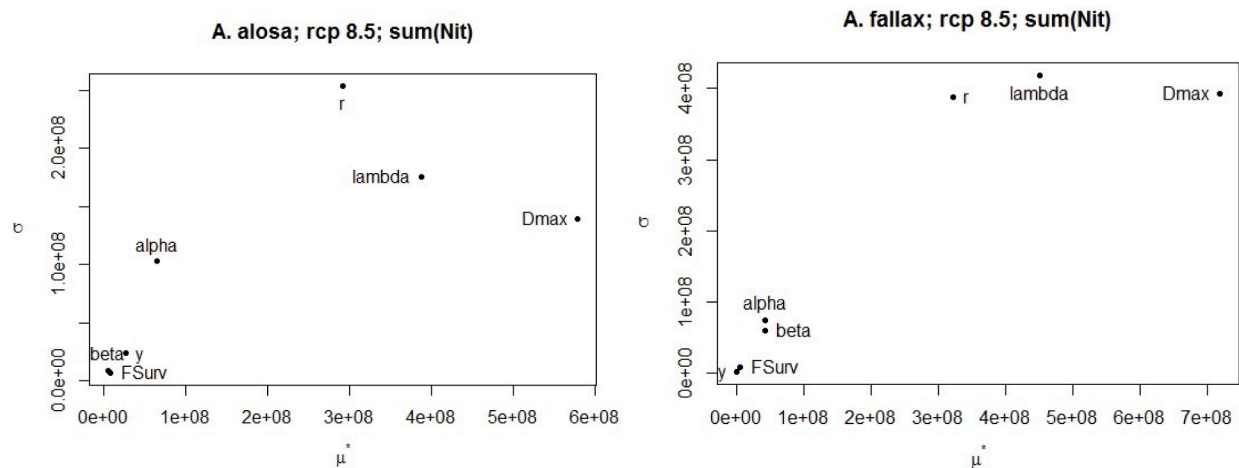
3.5. Model evaluation based on the saturation ratio metric

For allis shad, the shape of the saturation ratio distribution is bimodal at the extremes while a unique mode around 1 was depicted for twaite shad (Fig. 8). Regarding the confusion matrix between observed
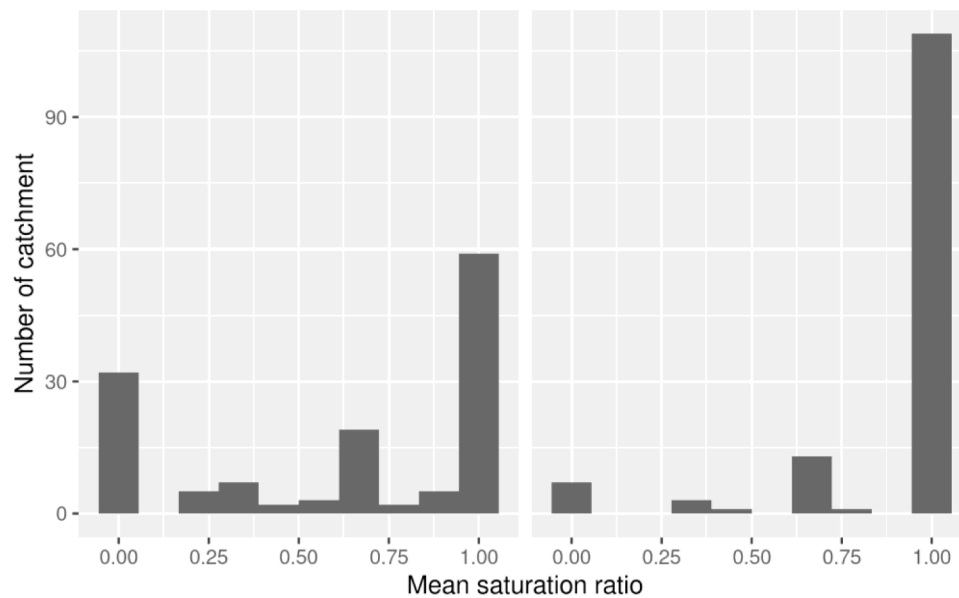
Fig. 6. Projections of saturation rate, spawner density and habitat suitability (HSI) averaged across three global climate models (GCMs) for *A. fallax* for different European catchments under climate scenario RCP 8.5 from 1951 to 2100. For heat plots, dark blue indicates smaller value and yellow indicates higher value. However, note difference in scale (indicated in legend) for the three heat plot panels. Fourth panel shows spawner abundance averaged for each catchment from 1951 to 1980 to provide a reference for a time horizon before populations started to change with climate change. Catchments are organized by country (indicated on left) and arranged within a country from north (top) to south. Individual catchment names are indicated on the right. See Appendix C for RCP4.5 results. (For interpretation of the references to colour in this figure legend, the reader is referred to the web version of this article.)

Fig. 7. Effect of model parameters on the estimate of total spawner abundance of shads summed across all catchments and years ($\sum N_{i,t}$). Results of global sensitivity analysis for *A. alosa* (left panel) and *A. fallax* (right panel). Parameters tested were *r* (population growth rate), λ (parameter for the Allee effect), D_{max} (maximum density of fish in ideal conditions), *y* (probability of emigration), α (scale parameter for the dispersal kernel), β (shape parameter for the dispersal kernel), and F_{Surv} (survival rate for emigrants during dispersal). Points are plotted with the average (μ^*) on the x-axis and the standard deviation (σ) of the elementary effects on the y-axis, which are calculated from trajectories that move through the parameter space varying one factor (X_i) *k* times (equal to the number of parameters). Twenty trajectories were performed to calculate the effect of each of the seven model parameters on the sum of spawner abundance.

Fig. 8. Distribution of the saturation ratios considering the three GCMs under RCP 8.5 for the period 2041–2050. The left and right panels were for *A. alosa* and *A. fallax* respectively.

abundance and $SR_{HSI=1}$, the error rate was 13 and 5.5% for allis and twaite shad respectively when considering as estimation errors only records above the diagonal. Errors in the upper half of the matrix indicated observed abundances that overpassed the saturation ratios calculated on the species maximum abundances without any anthropogenic pressures (Table 10).

4. Discussion

4.1. Development of the HyDiaD model

4.1.1. Novel approaches for the study of spatial dynamics in diadromous species

In this paper, we demonstrate for the first time how a hybrid model offers an alternative way to estimate spatial dynamics, thereby integrating how diadromous species move through a spatial matrix of

Table 10
Confusion matrix illustrating the agreement between observed and predicted abundance classes. In columns were given the observed abundance classes from EuroDiad 4.0 over the most recent period "2010-present times" and in rows the saturation ratio classes calculated with HyDiaD considering no anthropogenic pressures and a maximum habitat suitability (i.e. HSI = 1 in the SR denominator) over the period 2010–2019.

		Absent	Rare	Common	Abundant
A. alosa	SR = 0	12	1	5	
	[0; 0.333]	38	10	9	1
	[0.333; 0.667]	14	9	8	
	[0.667; 1]	6			1
A. fallax	SR = 0	6			
	[0; 0.333]	1	1	3	
	[0.333; 0.667]	18	5	2	3
	[0.667; 1]	25	18	24	4

catchments connected by the oceanic domain. As far we know, previous attempts at integrating multiple habitats are restricted to SDMs, so-called multi-state SDM (Frans et al., 2018), and this is the first time a multi-state habitat model has been coupled with population dynamics and dispersal processes in fish species. While the HyDiaD model was developed following the steps laid out by Singer et al. (2018) for hybrid species distribution models, several novel approaches were developed to address difficulties related to knowledge gaps and the fact that dispersal for diadromous species was measured between catchments that were different sizes and distances apart rather than through a continuous landscape, meaning it could not be estimated using the grid-cell approach often used for terrestrial species (De Cáceres and Brotons, 2012; Visintin et al., 2020). Even if this model is difficult to calibrate since it simulates a potential rather than an observable abundance, the confusion matrix between observed abundances provided by the Euro-Diad database and classes of simulated saturation ratios with HSI=1 showed a limited number of discrepancies (Table 10), leading to a quite good confidence in the model.

For data-poor species, the availability of species-specific data related to biological processes can be a major knowledge gap, and expert knowledge elicitation has been suggested as a possible solution (Gallien et al., 2010; Singer et al., 2018). The current study successfully used this approach on two aspects: i) to parameterize the HyDiaD model for two shad species (Section 2.3.4.), and ii) to fill data gaps related to both historical presences/absences and physical characteristics of catchments (Section 2.2.1). Lastly, given that marine predictor variables have been neglected in previous studies on diadromous species range-shift responses, the abiotic niche for the two shad species was estimated using a suite of environmental predictor variables that covered the entire species life cycle. The inclusion of marine and freshwater predictors led to high predictive accuracy when estimating habitat suitability for both species.

4.1.2. Applying HyDiaD to other species and geographic regions

The HyDiaD model could be applied to other anadromous species or modified to fit other life-history approaches such as catadromy, i.e. species that reproduce at sea and grow in rivers. For data-rich species, occupancy information and population and dispersal parameters could likely be found in the scientific literature, so the most time consuming process would likely be the downscaling of GCMs to the appropriate regional scale in order to obtain simulated data for environmental predictor variables. Another potential time-consuming process is the calculation of the distance matrix, which would require a longer computation time if a larger number of catchments were added. Increasing the number of catchments included in the calibration of the C-SDM will provide a better representation of the range of possible conditions that a species experiences and improve the estimation of habitat suitability.

The current study provides an approach for filling in knowledge gaps for data-poor diadromous species in which parameters for population and dispersal dynamics may not be readily available in the primary literature for the spatial scale used in the HyDiaD model. The use of iterative expert knowledge elicitation could be an alternative source of information in those cases. The results of the expert knowledge survey, in addition to the equations and R script for calculating the weighted group mean (Appendix A), could be used to apply the HyDiaD model to other diadromous species and geographic regions. However, the ecological processes behind the parameters being estimated are complex and the spatial scale covered by the model was large, thus extensive feedback was necessary to develop the wording of the questions used in the expert knowledge survey. To address this, the survey consisted of multiple rounds with a workshop in between to make sure that the survey questions were interpreted correctly by the respondents. After presenting the preliminary group results and discussing the survey questions in both the workshop and one-on-one interviews, many participants changed their initial answer to particular questions based on a

better understanding of what the authors intended to estimate. To further address this, future applications of this expert knowledge survey may benefit from two rounds of one-on-one interviews rather than an initial questionnaire followed by individual interviews.

While this kind of approach might be necessary in poor data situations, it has to be recognized that there are several potential pitfalls to consider when using this type of expert survey process. For example, there is the concern that subjectivity and speculation in the answers provided by experts may lead to biased results. In addition, it is important to consider the ecological paradigm implicit in estimating parameters as the HyDiaD model was developed to apply the same values for population and dispersal parameters across all populations, and catchment-scale differences were related to environmental conditions. In the current study, these biases were addressed by using a group of experts studying shads across a large spatial scale, multiple steps to the survey, and a weighting scheme for the results that allowed participants to rate the level of confidence they had in their answers for each species and question combination (Scolozzi and Geneletti, 2012), which allowed for a more precise weighting scheme in the calculation of group averages. Although there is evidence for rapid adaptive evolution of species in response to climate change (Lavergne et al., 2010), the hybrid model used in this study did not account for the adaptive potential of species, phenotypic plasticity, and ecological processes such as competition, positive interactions, and trophic relationship which can affect rates of species range shifts (Lavergne et al., 2010).

For data-poor species, finding historical presence/absence information can be difficult and time-consuming. In the current study, historical presence/absence information was available for the two shad species because of an existing database (https://data.inrae.fr/dataset.xhtml?persistentId=doi:10.15454/IVVAIC; Barber-O'Malley et al. (2022)). This database required enormous effort from a large group of students and project partners to create and validate, but this work will allow the HyDiaD model to be applied to other diadromous species both within the same area used in the current study as well as other areas in Europe. While many diadromous species historically supported a freshwater commercial fishery that should be a matter of public record, the temporal resolution of these data may be coarse. In addition, for species that are similar in appearance, it may be difficult to distinguish based on historical records whether one or both species were present, and making inferences based on the historic species range can reduce the fine-scale resolution of the occupancy data used to calibrate the C-SDM (e.g. Doadrio et al., 1991, 2011).

4.2. Using HyDiaD to estimate future projections of shad distributions

4.2.1. Habitat suitability

The trends seen in the estimate of habitat suitability and shifts in distribution for both shad species in the current study are similar to what was estimated by Lassalle et al. (2008b) and Lassalle and Rochard (2009) using C-SDMs, suggesting that habitat suitability may play a larger role than population dynamics and dispersal in the distribution of these two species. This point was also suggested by the dominance of saturation ratios close to 1 in the distributions across catchments indicating that variations in habitat suitability were quickly followed by changes in population abundances in relation with the relatively high specific population growth rates. In contrast to these previous two C-SDM studies, surface area only accounted for roughly 9% of the relative influence for both shad species in the current study, and precipitation (17.5% for *A. alosa* and 21.8% for *A. fallax*) and altitude at the source (16.9% for *A. alosa* and 18.1% for *A. fallax*), which together can act as a proxy for river flow (Lassalle and Rochard 2009; Pont et al., 2005), had a large influence. Mixed layer depth, which was not included in the previous studies, was also influential in the current study (21.6% for *A. alosa* and 11.5 for *A. fallax*), with a higher habitat suitability when mixed layer depth was lower. Studies on the Moroccan coast have suggested that shallow mixed layer depth corresponds to high cold-water

upwelling activity (Bessa et al., 2019), which could also lead to lower temperatures (Nykjær and Van Camp, 1994) and higher productivity and food availability in this region (Lassalle et al., 2008a).

Similar to the previous two studies, general distribution trends in the current study indicated that *A. fallax* is expected to increase in abundance and *A. alosa* is expected to decrease in abundance under XXIst century climate change scenarios. The current model estimated relatively high values of habitat suitability for *A. fallax* across its range. The lowest and most variable estimates for habitat suitability and spawner density for *A. fallax* were seen in catchments in southern Spain, southern Portugal, and northern Morocco. For *A. alosa*, the two previous studies predicted drastic declines in suitable habitat within the southern range of the species. In the current study, habitat suitability for *A. alosa* was consistently lower across catchments and more variable through the entire modeled timeframe (1951–2100), especially for basins in Spain, Portugal, and Morocco. For this species, some of the response curves used to estimate fitted values from the boosted regression trees were relatively steep for several of the environmental predictor variables, and this can result in a higher estimate of habitat suitability when there is only a relatively small change in the value of that variable. To address this, future applications of HyDiaD could include process-based habitat suitability model under the ecological niche theory framework (Citores et al., 2020), and to downplay the influence of these steep slopes on estimates of habitat suitability.

4.2.2. Dispersal

Dispersal parameters (probability of emigration and mortality rate for emigrants during dispersal) estimated from the expert knowledge survey indicated that long-distance dispersal events were rare for both shad species. This was supported in the literature by genetic and microchemistry studies that indicated shads displayed a high rate of natal homing (Alexandrino et al., 2006; ICES, 2015; Martin et al., 2015). High homing rates may decrease the ability of shads to adapt to climate-induced changes in habitat suitability by preventing populations from shifting their distribution take advantage of previously unoccupied habitat that becomes suitable.

However, despite the indication of natal homing, there is also evidence that suggests some dispersal of *A. alosa* between catchments that were as far apart as 2000 km (Randon et al., 2017), meaning that, while rare, long-distance dispersal does occur. Previous studies have indicated a lack of fine-scale genetic structure among nearby *A. alosa* populations (Alexandrino et al., 2006; Jolly et al., 2012; Martin et al., 2015), which may be the result of the small number of individuals that disperse longer distances. It is unlikely that many individuals disperse across very long distances, though, as genetic and morphological differences have been observed between populations in France and those in Portugal (Alexandrino et al., 2006; Lassalle et al., 2008a).

Previous studies have indicated that *A. fallax* has a higher level of genetic structure (ICES, 2015) and a greater rate of natal homing (Alexandrino et al., 2006; Jolly et al., 2012), which may limit its ability to colonize newly suitable habitats. Jolly et al. (2012) found that neighboring populations in the UK (Severn and Wye) displayed no genetic differentiation, while the Severn was genetically distinct from several populations located at a farther distance (Tywi, Usk, and Irish catchments). Davies et al. (2020) found that 33 out of 34 *A. fallax* tagged in 2018 from the Severn returned to this catchment in 2019. However, in tagging studies capture location may not represent natal origin (Nachón et al., 2020), and there may still be long distance dispersal between major estuaries (Davies et al., 2020).

For shads, not all river catchments in the European Atlantic area listed in the CCM River and Catchment Database (data.europa.eu) were included in the model projections. Many small and medium-sized catchments were not incorporated into the dispersal matrix because simulations only used catchments included in EuroDiad 4.0. In HyDiaD, smaller catchments would not produce a large number of dispersers because this value was based on an estimate of productivity directly related to surface area, and dispersal mortality applied using the distance between a pair of catchments. Out of the 18,769 pairwise distances in the dispersal matrix, only a small proportion (0.06% for *A. alosa* and 0.03% for *A. fallax*; Appendix D) were less than the maximum emigration distances estimated in the expert knowledge survey. So, while the dispersal kernel allowed a small proportion of emigrants to move past this maximum distance, these spawners did not survive to reach a further catchment. If the dispersal matrix included more catchments that were each a shorter distance away, it is possible that the resulting increase in the number and survival of dispersing spawners could allow surrounding catchments to be "rescued" from the Allee effect due to an annual influx of dispersing fish (Kanarek et al., 2015). Recent studies have suggested that small catchments could be more important for the resilience of diadromous species than previously thought (Melo-Merino et al., 2020; Copp et al., 2021), and so future applications of the HyDiaD model would benefit from the inclusion of more small catchments in future projections.

4.2.3. Disentangling habitat suitability and population and dispersal dynamics

It is difficult to disentangle the effects of habitat suitability on the estimates of spawner abundance from those of population and dispersal dynamics within a given catchment. Within the HyDiaD model, the Allee effect was imposed by reducing the number of spawners that were participating in reproduction within a given catchment. Potential demographic rescue from the Allee effect due to immigration was limited for both shad species because of interactions between dispersal capabilities, habitat suitability and annual stochasticity, population growth, a low proportion of spawners participating in reproduction, and the focus on medium and large-sized catchments included in the distance matrix. For both species, dispersal from a given population was low, and was generally restricted to nearby catchments. When environmental conditions were limiting, the number of spawners in a catchment were reduced to the point where recovery was not possible because the population could not surpass the threshold set by the Allee effect. If habitat suitability was low for several years within a short time period, spawner density decreased and was often unable to recover regardless of an increase in habitat suitability in later years. The combination of high habitat suitability, relatively high population growth rate, and low Allee effect allowed most *A. fallax* populations to persist. In contrast, many *A. alosa* populations experienced consistently low habitat suitability, and this led to low estimates of spawner density and many catchments with population crashes. This is demonstrated in the *A. alosa* population crashes early in the time series in catchments with very high annual variability in habitat suitability along the northern coast of Spain (Cantabrian coast). These rivers are generally short and steep with high water flow (Doadrio et al. (2011); Dr. David José Nachón García, personal communication), and while these catchments had spawners present at the start of the model simulation, indicating that the model was correctly simulating the presence/absence data used for calibration, these populations quickly dropped below the threshold imposed by the Allee effect and were unable to recover. Surrounding populations in Spain, Portugal, and France, either because of a low spawners abundance or too long of a long distance, were unable to produce enough dispersers for the Cantabrian populations to recover. This specific dynamics simulated in several catchments reinforce the need in new approaches that do not limit the interpretation to single-habitat suitability. This conclusion might become more apparent when considering species with a slower turnover rate as highlighted in the present study (Fig. 8) by the lower peak at SR =1 for allis shad than twaite shad (the former having a lower population growth rate than the latter). For such a group of species, regional dynamics driven by specific ecological and physical features will turn more frequent in the species range as not masked by the population ability in quickly recovering from unsuitable conditions, leading to question the underlying mechanisms.

4.3. Conclusion

The HyDiaD model was developed to estimate the distribution of diadromous species under climate scenarios, and was successfully applied to two shad species in the Atlantic Area of Europe. Estimated trends indicated that under XXIst century climate scenarios, habitat suitability for *A. fallax* is expected to increase, which would likely lead to an increase in abundance except possibly in the southernmost catchments of this species' current range in Morocco, Portugal, and Spain. Model estimates indicated that habitat suitability for *A. alosa* is expected to decrease, as well as display higher rates of annual variability, particularly in southern catchments. As anthropogenic factors were not modeled for the two shad species, these results may be exacerbated by problems with river connectivity or water pollution. Future studies can apply the HyDiaD model to other diadromous species, including data-poor ones, using species-specific estimates of population dynamics and dispersal parameters.

CRediT authorship contribution statement

Betsy Barber-O'Malley: Data curation, Validation, Formal analysis, Methodology, Writing – original draft. **Géraldine Lassalle:** Conceptualization, Methodology, Funding acquisition, Supervision, Writing – review & editing. **Guillem Chust:** Conceptualization, Methodology, Writing – review & editing. **Estibaliz Diaz:** Funding acquisition, Writing – review & editing. **Andrew O'Malley:** Methodology, Formal analysis, Writing – review & editing. **César Paradinas Blázquez:** Data curation, Validation. **Javier Pórtoles Marquina:** Data curation, Validation. **Patrick Lambert:** Conceptualization, Formal analysis, Methodology, Funding acquisition, Supervision, Writing – review & editing.

Declaration of Competing Interest

The authors declare that they have no known competing financial interests or personal relationships that could have appeared to influence the work reported in this paper.

Acknowledgements

Supplementary materials

Supplementary material associated with this article can be found, in the online version, at doi:10.1016/j.ecolmodel.2022.109997.

References

Allouche, O., Tsoar, A., Kadmon, R., 2006. Assessing the accuracy of species distribution models: prevalence, kappa and the true skill statistic (TSS). J. Appl. Ecol. 43, 1223–1232. https://doi.org/10.1111/j.1365-2664.2006.01214.x.

Aprahamian, M., Baglinière, J.-.L., Sabatié, R.M., Alexandrino, P., Thiel, R., Aprahamian, C.D., 2003. Biology, status and conservation of the anadromous Twaite shad *Alosa fallax fallax* (Lacépède, 1803). In: Limburg, K.E., Waldman, J.R. (Eds.), Biodiversity, status, and Conservation of the World's shads. American Fisheries Society, Baltimore, USA, pp. 103–124.

Baglinière, J.L., Sabatié, M.R., Rochard, E., Alexandrino, P.J., Aprahamian, M.W., 2003. The Allis shad (*Alosa alosa* Linneus, 1758): biology, ecology, range and status of populations. In: Limburg, K.E., Waldman, J.R. (Eds.), Biodiversity, status, and Conservation of the World's shads. American Fisheries Society, Baltimore, USA, pp. 85–102.

Barber-O'Malley, B., Lassalle, G., Lambert, P., Quinton, E., 2022. Dataset on European diadromous species distributions from 1750 to present time in Europe, North Africa and the Middle East. Data Brief 40, 107821. https://doi.org/10.1016/j.dib.2022.107821.

Barrowman, N.J., Myers, R.A., 2000. Still more spawner-recruitment curves: the hockey stick and its generalizations. Can. J. Fish. Aquat. Sci. 57, 665–676. https://doi.org/10.1139/f99-282.

Béguer, M., Beaulaton, L., Rochard, E., 2007. Distribution and richness of diadromous fish assemblages in Western Europe: large scale explanatory factors. Ecol. Freshw. Fish. 16, 221–237. https://doi.org/10.1111/j.1600-0633.2006.00214.x.

Bentsen, M., Bethke, I., Debernard, J.B., Iversen, T., Kirkevåg, A., Seland, Ø., Drange, H., Roelandt, C., Seierstad, I.A., Hoose, C., Kristjánsson, J.E., 2013. The Norwegian Earth System Model, NorESM1-M – Part 1: Description and basic evaluation of the physical climate. Geosci. Model Dev. 6, 687–720. https://doi.org/10.5194/gmd-6-687-2013.

Berec, L., 2019. Allee effects under climate change. Oikos 128, 972–983. https://doi.org/10.1111/oik.05941.

Bessa, I., Makaoui, A., Agouzouk, A., Idrissi, M., Hilmi, K., Afifi, M., 2019. Seasonal variability of the ocean mixed layer depth depending on the cape Ghir filament and the upwelling in the. Moroccan Atlantic coast. Materials Today: Proceedings 13, 637–645. https://doi.org/10.1016/j.matpr.2019.04.023.

Boulangeat, I., Gravel, D., Thuiller, W., 2012. Accounting for dispersal and biotic interactions to disentangle the drivers of species distributions and their abundances. Ecol. Lett. 15, 584–593. https://doi.org/10.1111/j.1461-0248.2012.01772.x.

Bowlby, H.D., Gibson, A.J.F., 2019. Evaluating whether metapopulation structure benefits endangered diadromous fishes. Can. J. Fish. Aquat. Sci. 77, 388–400. https://doi.org/10.1139/cjfas-2019-0001.

Bradie, J., Leung, B., 2017. A quantitative synthesis of the importance of variables used in MaxEnt species distribution models. J. Biogeogr. 44, 1344–1361. https://doi.org/10.1111/jbi.12894.

Bruge, A., Alvarez, P., Fontán, A., Cotano, U., Chust, G., 2016. Thermal niche tracking and future distribution of atlantic mackerel spawning in response to ocean warming. Front. Mar. Sci. 3 https://doi.org/10.3389/fmars.2016.00086.

Campolongo, F., Cariboni, J., Saltelli, A., 2007. An effective screening design for sensitivity analysis of large models. Environ. Model. Softw. 22, 1509–1518. https://doi.org/10.1016/j.envsoft.2006.10.004.

Casanueva, A., Kotlarski, S., Herrera, S., Fernández, J., Gutiérrez, J.M., Boberg, F., Colette, A., Christensen, O.B., Goergen, K., Jacob, D., Keuler, K., Nikulin, G., Teichmann, C., Vautard, R., 2016. Daily precipitation statistics in a EURO-CORDEX RCM ensemble: added value of raw and bias-corrected high-resolution simulations. Clim. Dyn. 47, 719–737. https://doi.org/10.1007/s00382-015-2865-x.

Chapman, D.S., Dytham, C., Oxford, G.S., 2007. Modelling population redistribution in a leaf beetle: an evaluation of alternative dispersal functions. J. Anim. Ecol. 76, 36–44. https://doi.org/10.1111/j.1365-2656.2006.01172.x.

Cheung, W.W.L., Lam, V.W.Y., Sarmiento, J.L., Kearney, K., Watson, R., Zeller, D., Pauly, D., 2010. Large-scale redistribution of maximum fisheries catch potential in the global ocean under climate change. Glob. Change Biol. 16, 24–35. https://doi.org/10.1111/j.1365-2486.2009.01995.x.

Citores, L., Ibaibarriaga, L., Lee, D.J., Brewer, M.J., Santos, M., Chust, G., 2020. Modelling species presence–absence in the ecological niche theory framework using shape-constrained generalized additive models. Ecol. Model. 418, 108926 https://doi.org/10.1016/j.ecolmodel.2019.108926.

Copp, G.H., Daverat, F., Bašić, T., 2021. The potential contribution of small coastal streams to the conservation of declining and threatened diadromous fishes, especially the European eel. River Res. Appl. 37, 111–115. https://doi.org/10.1002/rra.3746.

Costa-Dias, S., Sousa, R.S., Lobón-Cerviá, J., Laffaille, P., 2009. The decline of diadromous fish in Western Europe inland waters: mains causes and consequence. In: McManus, N.F., Bellinghouse, D.S. (Eds.), Fisheries: Management, Economics and Perspectives. Nova Science Publishers, pp. 67–92.

Dambach, J., Rödder, D., 2011. Applications and future challenges in marine species distribution modeling. Aquat. Conserv. Mar. Freshw. Ecosys. 21, 92–100. https://doi.org/10.1002/aqc.1160.

Davies, P., Britton, R.J., Nunn, A.D., Dodd, J.R., Crundwell, C., Velterop, R., Ó'Maoiléidigh, N., O'Neill, R., Sheehan, E.V., Stamp, T., Bolland, J.D., 2020. Novel insights into the marine phase and river fidelity of anadromous twaite shad *Alosa fallax* in the UK and Ireland. Aquat. Conserv. Mar. Freshw. Ecosys. 30, 1291–1298. https://doi.org/10.1002/aqc.3343.

De'ath, G., 2007. Boosted trees for ecological modeling and prediction. Ecology 88, 243–251. https://doi.org/10.1890/0012-9658(2007)88[243:BTFEMA]2.0.CO;2.

De Cáceres, M., Brotons, L., 2012. Calibration of hybrid species distribution models: the value of general-purpose vs. targeted monitoring data. Divers. Distrib. 18, 977–989. https://doi.org/10.1111/j.1472-4642.2012.00899.x.

Doadrio, I., Elvira, B., Bernat, Y., 1991. Peces continentales espanoles - Inventario y clasificacion de zonas fluviales. ICONA 221.

Doadrio, I., Perea, S., Garzón-Heydt, P., González, J.L., 2011. Ictiofauna Continental española: Bases Para Su Seguimiento. DG Medio Natural y Política Forestal, Madrid, Spain, p. 616.

Dormann, C.F., Schymanski, S.J., Cabral, J., Chuine, I., Graham, C., Hartig, F., Kearney, M., Morin, X., Römermann, C., Schröder, B., Singer, A., 2012. Correlation and process in species distribution models: bridging a dichotomy. J. Biogeogr. 39, 2119–2131. https://doi.org/10.1111/j.1365-2699.2011.02659.x.

Elith, J., Leathwick, J.R., Hastie, T., 2008. A working guide to boosted regression trees. J. Anim. Ecol. 77, 802–813. https://doi.org/10.1111/j.1365-2656.2008.01390.x.

Elith, J., Kearney, M., Phillips, S., 2010. The art of modelling range-shifting species. Methods Ecol. Evol. 1, 330–342. https://doi.org/10.1111/j.2041-210X.2010.00036.x.

Elith, J., Phillips, S.J., Hastie, T.J., Dudík, M., Chee, Y.E., Yates, C.J., 2011. A statistical explanation of MaxEnt for ecologists. Divers. Distrib. 17, 43–57. https://doi.org/10.1111/j.1472-4642.2010.00725.x.

Elmer, F., Seifert, I., Kreibich, H., Thieken, A.H., 2010. A delphi method expert survey to derive standards for flood damage data collection. Risk Anal. 30, 107–124. https://doi.org/10.1111/j.1539-6924.2009.01325.x.

Erauskin-Extramiana, M., Arrizabalaga, H., Hobday, A.J., Cabré, A., Ibaibarriaga, L., Arregui, I., Murua, H., Chust, G., 2019. Large-scale distribution of tuna species in a warming ocean. Glob. Change Biol. 25, 2043–2060. https://doi.org/10.1111/gcb.14630.

Fielding, A.H., Bell, J.F., 1997. A review of methods for the assessment of predictor error in conservation presence/absence models. Environ. Conserv. 24, 38–49. https://doi.org/10.1017/S0376892997000088.

Fordham, D.A., Bertelsmeier, C., Brook, B.W., Early, R., Neto, D., Brown, S.C., Ollier, S., Araújo, M.B., 2018. How complex should models be? Comparing correlative and mechanistic range dynamics models. Glob. Change Biol. 24, 1357–1370. https://doi.org/10.1111/gcb.13935.

Fordham, D.A., Mellin, C., Russell, B.D., Akckaya, R.H., Bradshaw, C.J.A., Aiello-Lammens, M.E., Caley, J.M., Connell, S.D., Mayfield, S., Sheperd, S.A., Brook, B.W., 2013. Population dynamics can be more important than physiological limits for determining range shifts under climate change. Glob. Change Biol. 19, 3224–3237. https://doi.org/10.1111/gcb.12289.

Franczyk, A., 2019. Using the Morris sensitivity analysis method to assess the importance of input variables on time-reversal imaging of seismic sources. Acta Geophys. 67, 1525–1533. https://doi.org/10.1007/s11600-019-00356-5.

Franklin, J., 2010. Moving beyond static species distribution models in support of conservation biogeography. Divers. Distrib. 16, 321–330. https://doi.org/10.1111/j.1472-4642.2010.00641.x.

Frans, V.F., Augé, A.A., Edelhoff, H., Erasmi, S., Balkenhol, N., Engler, J.O., 2018. Quantifying apart what belongs together: A multi-state species distribution modelling framework for species using distinct habitats. Methods Ecol. Evol. 9, 98–108. https://doi.org/10.1111/2041-210X.12847.

Friedman, J.H., 2001. Greedy function approximation: A gradient boosting machine. Ann. Stat. 29, 1189–1232. https://doi.org/10.1214/aos/1013203451.

Gallien, L., Münkemüller, T., Albert, C.H., Boulangeat, I., Thuiller, W., 2010. Predicting potential distributions of invasive species: where to go from here? Divers. Distrib. 16, 331–342. https://doi.org/10.1111/j.1472-4642.2010.00652.x.

Gotelli, N.J., 1991. Metapopulation models: The rescue effect, the propagule rain, and the core-satellite hypothesis. Am. Nat. 138, 768–776. https://doi.org/10.1086/285249.

Greenwell, B., Boehmke, B., Cunningham, J., Developers, G., 2020. Package "gbm": generalized boosted regression models. R package version 2.1.8.

Gu, Z., Eils, R., Schlesner, M., 2016. Complex heatmaps reveal patterns and correlations in multidimensional genomic data. Bioinformatics 32, 2847–2849. https://doi.org/10.1093/bioinformatics/btw313.

Guisan, A., Zimmermann, N.E., 2000. Predictive habitat distribution models in ecology. Ecol. Model. 135, 147–186. https://doi.org/10.1016/S0304-3800(00)00354-9.

Guisan, A., Thuiller, W., 2005. Predicting species distribution: offering more than simple habitat models. Ecol. Lett. 8, 993–1009. https://doi.org/10.1111/j.1461-0248.2005.00792.x.

Hanski, I., 1994. A practical model of metapopulation dynamics. J. Anim. Ecol. 63, 151–162. https://doi.org/10.2307/5591.

Hanski, I., 1998. Metapopulation dynamics. Nature 396, 41–49. https://doi.org/10.1038/23876.

Hare, J.A., Morrison, W.E., Nelson, M.W., Stachura, M.M., Teeters, E.J., Griffis, R.B., Alexander, M.A., Scott, J.D., Alade, L., Bell, R.J., Chute, A.S., Curti, K.L., Curtis, T.H., Kircheis, D., Kocik, J.F., Lucey, S.M., McCandless, C.T., Milke, L.M., Richardson, D. E., Robillard, E., Walsh, H.J., McManus, M.C., Marancik, K.E., Griswold, C.A., 2016. A vulnerability assessment of fish and invertebrates to climate change on the Northeast U.S. continental shelf. PLoS ONE 11, e0146756. https://doi.org/10.1371/journal.pone.0146756.

Harris, R.M.B., Grose, M.R., Lee, G., Bindoff, N.L., Porfirio, L.L., Fox-Hughes, P., 2014. Climate projections for ecologists. WIREs Clim. Change 5, 621–637. https://doi.org/10.1002/wcc.291.

Harrison, S., 1991. Local extinction in a metapopulation context: an empirical evaluation. Biol. J. Linn. Soc. 42, 73–88. https://doi.org/10.1111/j.1095-8312.1991.tb00552.x.

Hijmans, R.J., Phillips, S., Leathwick, J.R., Elith, J., 2021. Package "dismo": species distribution model. R package version 1.3-5.

Holloway, P., Miller, J.A., 2017. A quantitative synthesis of the movement concepts used within species distribution modelling. Ecol. Model. 356, 91–103. https://doi.org/10.1016/j.ecolmodel.2017.04.005.

Hutchings, J.A., 2014. Renaissance of a caveat: Allee effects in marine fish. ICES J. Mar. Sci. 71, 2152–2157. https://doi.org/10.1093/icesjms/fst179.

ICES, 2015. Report of the Workshop On Lampreys and Shads (WKLS), p. 206, 27–29 November 2014, Lisbon, Portugal.

Iooss, B., Da Veiga, S., Janon, A., Pujol, G., 2021. Package "sensitivity": global sensitivity analysis of model outputs. R package version 1.27.0.

Iversen, T., Bentsen, M., Bethke, I., Debernard, J.B., Kirkevåg, A., Seland, Ø., Drange, H., Kristjansson, J.E., Medhaug, I., Sand, M., Seierstad, I.A., 2013. The Norwegian Earth System Model, NorESM1-M – Part 2: Climate response and scenario projections. Geosci. Model Dev. 6, 389–415. https://doi.org/10.5194/gmd-6-389-2013.

Jacob, D., Petersen, J., Eggert, B., Alias, A., Christensen, O.B., Bouwer, L.M., Braun, A., Colette, A., Déqué, M., Georgievski, G., Georgopoulou, E., Gobiet, A., Menut, L., Nikulin, G., Haensler, A., Hempelmann, N., Jones, C., Keuler, K., Kovats, S., Kröner, N., Kotlarski, S., Kriegsmann, A., Martin, E., van Meijgaard, E., Moseley, C., Pfeifer, S., Preuschmann, S., Radermacher, C., Radtke, K., Rechid, D., Rounsevell, M., Samuelsson, P., Somot, S., Soussana, J.-F., Teichmann, C., Valentini, R., Vautard, R., Weber, B., Yiou, P., 2014. EURO-CORDEX: new high-resolution climate change projections for European impact research. Reg. Environ. Change 14, 563–578. https://doi.org/10.1007/s10113-013-0499-2.

Jaeschke, A., Bittner, T., Reineking, B., Beierkuhnlein, C., 2013. Can they keep up with climate change? – Integrating specific dispersal abilities of protected Odonata in species distribution modelling. Insect. Conserv. Divers. 6, 93–103. https://doi.org/10.1111/j.1752-4598.2012.00194.x.

Jolly, M.T., Aprahamian, M.W., Hawkins, S.J., Henderson, P.A., Hillman, R., O'Maoiléidigh, N., Maitland, P.S., Piper, R., Genner, M.J., 2012. Population genetic structure of protected allis shad (*Alosa alosa*) and twaite shad (*Alosa fallax*). Mar. Biol. 159, 675–687. https://doi.org/10.1007/s00227-011-1845-x.

Kanarek, A.R., Webb, C.T., Barfield, M., Holt, R.D., 2015. Overcoming Allee effects through evolutionary, genetic, and demographic rescue. J. Biol. Dyn. 9, 15–33. https://doi.org/10.1080/17513758.2014.978399.

Kearney, M.R., Porter, W., 2009. Mechanistic niche modelling: combining physiological and spatial data to predict species ranges. Ecol. Lett. 12, 334–350. https://doi.org/10.1111/j.1461-0248.2008.01277.x.

Kotlarski, S., Keuler, K., Christensen, O.B., Colette, A., Déqué, M., Gobiet, A., Goergen, K., Jacob, D., Lüthi, D., van Meijgaard, E., Nikulin, G., Schär, C., Teichmann, C., Vautard, R., Warrach-Sagi, K., Wulfmeyer, V., 2014. Regional climate modeling on European scales: a joint standard evaluation of the EURO-CORDEX RCM ensemble. Geosci. Model Dev. 7, 1297–1333. https://doi.org/10.5194/gmd-7-1297-2014.

Kottelat, M., Freyhof, J., 2007. Handbook of European freshwater Fishes. Kottelat, Cornol, Switzerland and Freyhof, Berlin, Germany, p. 646.

Kuparinen, A., Keith, D.M., Hutchings, J.A., 2014. Allee effect and the uncertainty of population recovery. Conserv. Biol. 28, 790–798. https://doi.org/10.1111/cobi.12216.

Landis, J.R., Koch, G.G., Lawton, J., 1977. The measurements of observer agreement for categorical data. Biometrics 33, 159–174.

Lassalle, G., Rochard, E., 2009. Impact of twenty-first century climate change on diadromous fish spread over Europe, North Africa and the Middle East. Glob. Change Biol. 15, 1072–1089. https://doi.org/10.1111/j.1365-2486.2008.01794.x.

Lassalle, G., Trancart, T., Lambert, P., Rochard, E., 2008a. Latitudinal variations in age and size at maturity among allis shad Alosa alosa populations. J. Fish Biol. 73, 1799–1809. https://doi.org/10.1111/j.1095-8649.2008.02043.x.

Lassalle, G., Béguer, M., Beaulaton, L., Rochard, E., 2008b. Diadromous fish conservation plans need to consider global warming issues: an approach using biogeographical models. Biol. Cons. 141, 1105–1118. https://doi.org/10.1016/j.biocon.2008.02.010.

Lassalle, G., Crouzet, P., Gessner, J., Rochard, E., 2010. Global warming impacts and conservation responses for the critically endangered European Atlantic sturgeon. Biol. Cons. 143, 2441–2452. https://doi.org/10.1016/j.biocon.2010.06.008.

Latimer, A.M., Wu, S., Gelfand, A.E., Silander Jr, J.A., 2006. Building statistical models to analyze species distributions. Ecol. Appl. 16, 33–50. https://doi.org/10.1890/04-0609.

Lavergne, S., Mouquet, N., Thuiller, W., Ronce, O., 2010. Biodiversity and climate change: Integrating evolutionary and ecological responses of species and communities. Annu. Rev. Ecol. Evol. Syst. 41, 321–350. https://doi.org/10.1146/annurev-ecolsys-102209-144628.

Limburg, K., Waldman, J.R., 2009. Dramatic declines in North Atlantic diadromous fishes. Bioscience 59, 955–965. https://doi.org/10.1525/bio.2009.59.11.7.

Lin, H.-Y., Bush, A., Linke, S., Possingham, H.P., Brown, C.J., 2017. Climate change decouples marine and freshwater habitats of a threatened migratory fish. Divers. Distrib. 23, 751–760. https://doi.org/10.1111/ddi.12570.

Lotze, H.K., Tittensor, D.P., Bryndum-Buchholz, A., Eddy, T.D., Cheung, W.W.L., Galbraith, E.D., Barange, M., Barrier, N., Bianchi, D., Blanchard, J.L., Bopp, L., Büchner, M., Bulman, C.M., Carozza, D.A., Christensen, V., Coll, M., Dunne, J.P., Fulton, E.A., Jennings, S., Jones, M.C., Mackinson, S., Maury, O., Niiranen, S., Oliveros-Ramos, R., Roy, T., Fernandes, J.A., Schewe, J., Shin, Y.-J., Silva, T.A.M., Steenbeek, J., Stock, C.A., Verley, P., Volkholz, J., Walker, N.D., Worm, B., 2019. Global ensemble projections reveal trophic amplification of ocean biomass declines with climate change. Proc. Natl. Acad. Sci. U. S. A. 116, 12907–12912. https://doi.org/10.1073/pnas.1900194116.

Martin, J., Rougemont, Q., Drouineau, H., Launey, S., Jatteau, P., Bareille, G., Berail, S., Pécheyran, C., Feunteun, E., Roques, S., Clavé, D., Nachón, D.J., Antunes, C., Mota, M., Réveillac, E., Daverat, F., 2015. Dispersal capacities of anadromous Allis shad population inferred from a coupled genetic and otolith approach. Can. J. Fish. Aquat. Sci. 72, 991–1003. https://doi.org/10.1139/cjfas-2014-0510.

McDowall, R.M., 1988. Diadromy in Fishes - Migrations between Freshwater and Marine Environments. Croom Helm, London, UK, p. 308.

Melo-Merino, S.M., Reyes-Bonilla, H., Lira-Noriega, A., 2020. Ecological niche models and species distribution models in marine environments: A literature review and spatial analysis of evidence. Ecol. Model. 415, 108837 https://doi.org/10.1016/j. ecolmodel.2019.108837.

Mitchell, T.D., Jones, P.D., 2005. An improved method of constructing a database of monthly climate observations and associated high-resolution grids. Int. J. Climatol. 25, 693–712. https://doi.org/10.1002/joc.1181.

Morris, M.D., 1991. Factorial sampling plans for preliminary computational experiments. Technometrics 33, 161–174. https://doi.org/10.1080/00401706.1991.10484804.

Nachón, D.J., Mota, M., Antunes, C., Servia, M.J., Cobo, F., 2016. Marine and continental distribution and dynamic of the early spawning migration of twaite shad (*Alosa fallax* (Lacépède, 1803)) and allis shad (*Alosa alosa* (Linnaeus, 1758)) in the north-west of the Iberian Peninsula. Mar. Freshw. Res. 67, 1229–1240. https://doi.org/10.1071/MF14243.

Nachón, D.J., Bareille, G., Drouineau, H., Tabouret, H., Taverny, C., Boisneau, C., Berail, S., Pécheyran, C., Claverie, F., Daverat, F., 2020. 1980s population-specific compositions of two related anadromous shad species during the oceanic phase determined by microchemistry of archived otoliths. Can. J. Fish. Aquat. Sci. 77, 164–176. https://doi.org/10.1139/cjfas-2018-0444.

Nykjær, L., Van Camp, L., 1994. Seasonal and interannual variability of coastal upwelling along northwest Africa and Portugal from 1981 to 1991. J. Geophys. Res. Oceans 99, 14197–14207. https://doi.org/10.1029/94JC00814.

Perälä, T., Kuparinen, A., 2017. Detection of Allee effects in marine fishes: analytical biases generated by data availability and model selection. Proc. R. Soc. Lond. B Biol. Sci. 284, 20171284 https://doi.org/10.1098/rspb.2017.1284.

Perry, A.L., Low, P.J., Ellis, J.R., Reynolds, J.D., 2005. Climate change and distribution shifts in marine fishes. Science 308, 1912–1915. https://doi.org/10.1126/science.1111322.

Phipps, S.J., Rotstayn, L.D., Gordon, H.B., Roberts, J.L., Hirst, A.C., Budd, W.F., 2011. The CSIRO Mk3L climate system model version 1.0 – Part 1: Description and evaluation. Geosci. Model Dev. 4, 483–509. https://doi.org/10.5194/gmd-4-483-2011.

Phipps, S.J., Rotstayn, L.D., Gordon, H.B., Roberts, J.L., Hirst, A.C., Budd, W.F., 2012. The CSIRO Mk3L climate system model version 1.0 – Part 2: Response to external forcings. Geosci. Model Dev. 5, 649–682. https://doi.org/10.5194/gmd-5-649-2012.

Pont, D., Hugueny, B., Oberdorff, T., 2005. Modelling habitat requirement of European fishes: do species have similar responses to local and regional environmental constraints? Can. J. Fish. Aquat. Sci. 62, 163–173. https://doi.org/10.1139/f04-183.

Quignard, J.-.P., Douchement, C., 1991. *Alosa Fallax Fallax* (Lacepede 1803). The Freshwater Fishes of Europe - Clupeidae. Anguillidae, Aula-Verlag, Wiesbaden, pp. 225–253.

Quinn, T.P., 1993. A review of homing and straying of wild and hatchery-produced salmon. Fish. Res. 18, 29–44. https://doi.org/10.1016/0165-7836(93)90038-9.

R Core Team, 2020. R: A language and Environment For Statistical Computing. R Foundation for Statistical Computing, Vienna, Austria.

Randon, M., Daverat, F., Bareille, G., Jatteau, P., Martin, J., Pecheyran, C., Drouineau, H., 2017. Quantifying exchanges of Allis shads between river catchments by combining otolith microchemistry and abundance indices in a Bayesian model. ICES J. Mar. Sci. https://doi.org/10.1093/icesjms/fsx148 fsx148-fsx148.

Robinson, L.M., Elith, J., Hobday, A.J., Pearson, R.G., Kendall, B.E., Possingham, H.P., Richardson, A.J., 2011. Pushing the limits in marine species distribution modelling: lessons from the land present challenges and opportunities. Glob. Ecol. Biogeogr. 20, 789–802. https://doi.org/10.1111/j.1466-8238.2010.00636.x.

Rougier, T., Drouineau, H., Dumoulin, N., Defuant, G., Rochard, E., Lambert, P., 2014. The GR3D model, a tool to explore the global repositioning dynamics of diadromous fish distribution. Ecol. Model. 283, 31–44. https://doi.org/10.1016/j. ecolmodel.2014.03.019.

Rougier, T., Lambert, P., Drouineau, H., Girardin, M., Castelnaud, G., Carry, L., Aprahamian, M.W., Rivot, E., Rochard, E., 2012. Collapse of Allis shad, *Alosa alosa*, in the Gironde system (southwest France): environmental change, fishing mortality, or Allee effect? ICES J. Mar. Sci. 69, 1802–1811. https://doi.org/10.1093/icesjms/fss149.

Schtickzelle, N., Quinn, T.P., 2007. A metapopulation perspective for salmon and other anadromous fish. Fish Fish 8, 297–314. https://doi.org/10.1111/j.1467-2979.2007.00256.x.

Scolozzi, R., Geneletti, D., 2012. Assessing habitat connectivity for land-use planning: a method integrating landscape graphs and Delphi survey. J. Environ. Plan. Manage. 55, 813–830. https://doi.org/10.1080/09640568.2011.628823.

Segurado, P., Branco, P., Avelar, A.P., Ferreira, M.T., 2015. Historical changes in the functional connectivity of rivers based on spatial network analysis and the past occurrences of diadromous species in Portugal. Aquat. Sci. 77, 427–440. https://doi.org/10.1007/s00027-014-0371-6.

Singer, A., Schweiger, O., Kühn, I., Johst, K., 2018. Constructing a hybrid species distribution model from standard large-scale distribution data. Ecol. Model. 373, 39–52. https://doi.org/10.1016/j.ecolmodel.2018.02.002.

Singer, A., Johst, K., Banitz, T., Fowler, M.S., Groeneveld, J., Gutiérrez, A.G., Hartig, F., Krug, R.M., Liess, M., Matlack, G., Meyer, K.M., Pe'er, G., Radchuk, V., Voinopol-Sassu, A.-.J., Travis, J.M.J., 2016. Community dynamics under environmental change: How can next generation mechanistic models improve projections of species distributions? Ecol. Model. 326, 63–74. https://doi.org/10.1016/j.ecolmodel.2015.11.007.

Steffen, W., Broadgate, W., Deutsch, L., Gaffney, O., Ludwig, C., 2015. The trajectory of the Anthropocene: The Great Acceleration. Anthr. Rev. 2, 81–98. https://doi.org/10.1177/2053019614564785.

Stephens, P.A., Sutherland, W.J., 1999. Consequences of the Allee effect for behaviour, ecology and conservation. Trends Ecol. Evol. 14, 401–405. https://doi.org/10.1016/S0169-5347(99)01684-5.

Swets, K., 1988. Measuring the accuracy of diagnostic systems. Science 240, 1285–1293. https://doi.org/10.1126/science.3287615.

Visintin, C., Briscoe, N.J., Woolley, S.N.C., Lentini, P.E., Tingley, R., Wintle, B.A., Golding, N., 2020. steps: Software for spatially and temporally explicit population simulations. Methods Ecol. Evol. 11, 596–603. https://doi.org/10.1111/2041-210X.13354.

Voldoire, A., Sanchez-Gomez, E., Salas y Mélia, D., Decharme, B., Cassou, C., Sénési, S., Valcke, S., Beau, I., Alias, A., Chevallier, M., Déqué, M., Deshayes, J., Douville, H., Fernandez, E., Madec, G., Maisonnave, E., Moine, M.P., Planton, S., Saint-Martin, D., Szopa, S., Tyteca, S., Alkama, R., Belamari, S., Braun, A., Coquart, L., Chauvin, F., 2013. The CNRM-CM5.1 global climate model: description and basic evaluation. Clim. Dyn. 40, 2091–2121. https://doi.org/10.1007/s00382-011-1259-y.

Whitehead, P.J.P., 1985. An annotated and illustrated catalogue of the herrings, sardines, pilchards, sprats, shads, anchovies, and wolf-herrings - Part 1 - Chirocentridae, Clupeidae and Pristigasteridae. 303 pp.

Wilson, K., Veneranta, L., 2019. Data-limited diadromous species – review of European status. 273 pp.

Winter, A.-.M., Richter, A., Eikeset, A.M., 2020. Implications of Allee effects for fisheries management in a changing climate: evidence from Atlantic cod. Ecol. Appl. 30, e01994. https://doi.org/10.1002/eap.1994.

Yang, C., Masina, S., Storto, A., 2017. Historical ocean reanalyses (1900–2010) using different data assimilation strategies. Q. J. R. Meteorol. Soc. 143, 479–493. https://doi.org/10.1002/qj.2936.